To the Graduate Council:

I am submitting herewith a thesis written by Kislaya Gautam entitled "Characterization of Heavy Oil Fractions Using Spectrometric Techniques". I have examined the final copy of this thesis for form and content and recommend that it be accepted in partial fulfillment of the requirement for the degree of Master of Science, with a major in Chemical Engineering.

Marion G. Hansen, Major Professor

We have read this thesis
and recommend its acceptance:

Accepted for the Council:

Associate Vice Chancellor and
Dean of The Graduate School

Characterization of Heavy Oil Fractions Using Spectrometric Techniques

A Thesis
Presented for the
Master of Science
Degree
The University of Tennessee, Knoxville

Kislaya Gautam
May 2000

Dedication

This work is dedicated to my nani

Mrs. Shakuntala Sinha

who has inspired me at all times in my life.

No university can offer the education that

I gained from her influence and upbringing.

Acknowledgments

The author wishes to express his gratitude to his major professor, Dr. Marion G. Hansen for his guidance and encouragement throughout the course of the thesis work. The author is grateful to Dr. John Coates, Top Source Instruments Inc. for providing the instrumentations and above all for giving helpful insights in the work. The author is indebted to his committee members, Dr. P. D. Frymier and Dr. R. M. Counce for all their assistance during his stay at the University of Tennessee. The author wishes to thank all his lab colleagues, Bhushan Deshpande, Jigui Li, Mrunalini Dhamdhere, and Parag Patil. The author is thankful to Betty Frazier, Sancy Hail, Frank Holiway, Randy Stookesbury, Doug Fielden, and Larry Smith. Without their help, this work would have faced many obstacles. Last but not the least, the author acknowledges the Laurel batallion for making his stay in Knoxville a very memorable one.

Abstract

The work presented in this thesis was focused on developing spectroscopic techniques that can be easily incorporated in an instrument for the rapid characterization of heavy oil fractions. Transmission infrared, attenuated total reflectance infrared, visible, and nuclear magnetic resonance spectroscopy were the techniques studied in the course of this project. The key properties of the heavy petroleum fraction that were characterized are as follows:

- Viscosity parameters: Viscosity at 210 and 100 ^{0}F, Viscosity Index
- Compositional: Relative percentage content of paraffin, naphthene, and aromatic
- Optical: Color of the heavy oil fraction

The techniques developed in this project would reduce the labor and maintenance involved in the quality control labs in the industry. The time scale of characterization by these techniques is of the order of 4 minutes and hence, the results can be used more effectively for process feedback. This is in stark contrast to the time taking characterization techniques prevalent in the industry. The following are the outcome of the project:

- The transmission Infrared (IR) is inappropriate for predicting the heavy oil properties

- Attenuated Total Reflectance (ATR) Infrared (IR) measurement is better for the present purposes
- Predictions of key viscosity parameters of the heavy oil fraction (Viscosity at 100 and 210 ^{0}F, and Viscosity Index) based on ATR IR measurements are good
- ATR IR spectra also correlated well with the compositional properties (percentage paraffin, naphthene, and aromatic) of the heavy oil fractions derived from the Nuclear Magnetic Resonance (NMR) spectra of the oil fractions
- For color characterization, IR spectrum was found inadequate. Visible spectra of the samples was found to be more useful for color characterization

The findings from the project suggest that a combination of ATR IR and visible spectroscopic measurement technique can successfully characterize the properties of heavy oil fractions. In future, these methods of analysis can be formalized into procedures transferable to a prototype analyzer.

Table of Contents

Chapter			Page
1.	Petroleum Chemistry		1
	1.1 Introduction		1
	1.2 Chemical Composition		2
	1.2.1 Hydrocarbon Components		4
		1.2.1.1 Paraffins	4
		1.2.1.2 Naphthenes	4
		1.2.1.3 Aromatics	5
	1.2.2 Non-hydrocarbon Components		5
		1.2.2.1 Sulfur	6
		1.2.2.2 Nitrogen	7
		1.2.2.3 Oxygen	7
	1.3 Crude Oil Distillation		7
	1.4 Petroleum Products		10
	1.4.1 Gas		11
	1.4.2 Gasoline		11
	1.4.3 Petroleum Solvents		12
	1.4.4 Kerosene		13
	1.4.5 Fuel Oils		14
	1.4.6 Lubricating Oil		14
	1.4.7 Waxes		15
2.	Petroleum Characterization		17
	2.1 Importance		17
	2.2 Important Oil Characteristics		19
	2.2.1 Composition		20
	2.2.2 Specific Gravity		20

2.2.3 Viscosity 21
2.2.4 Viscosity Index 22
2.2.5 Flash Point 22
2.2.6 Color 23
2.3 Overview of Characterization Techniques for Petroleum 24

3. Research Objective 27

4. Overview of the Spectroscopic and Quantitative Techniques 30
4.1 Principles of Electronic Spectroscopy 30
4.1.1 Origin of Electronic Spectroscopy 32
4.1.2 Features of Electronic Transitions 36
4.2 Principles of Vibrational Spectroscopy 37
4.2.1 Nature and Origin of Infrared Spectrum 38
4.2.2 Quantum Treatment of Vibrations 39
4.2.3 Spectral Assignment in Infrared 44
4.2.4 Sampling Techniques in Infrared Spectroscopy 44
4.2.4.1 Transmission Spectroscopy 48
4.2.4.2 Attenuated Total Reflectance 49
4.3 Nuclear Magnetic Resonance (NMR) Spectroscopy 52
4.3.1 Theory of NMR 52
4.4 Quantitative Techniques 56
4.4.1 Exploratory Data Analysis-Principal Component Analysis 57
4.4.2 Partial Component Regression and Partial Least Square Regression 61
4.4.3 Diagnostics of PCR and PLS Models 65

5. Review of Spectrometric Techniques for Characterization of Crude Oil And Petroleum Products 69
5.1 Crude Oil and Shale Oil 69
5.2 Fuel Fractions (gasoline, diesel, and kerosene) 72
5.3 Lube Oil 77
5.4 Heavy Fractions 79
5.5 Conclusions 83

6. Experimentation and Analysis 87
6.1 Background 87
6.2 Sample Description 92
6.3 Test Run on OSA-R Analyzer 94
6.3.1 Performance of the Original OSA-R Analyzer 94
6.3.2 Remodeling of the Chemometrics of OSA-R Analyzer 94
6.3.3 Modification in the Optical Cell of the OSA-R Analyzer 105
6.4 ATR IR Sampling Technique 116
6.4.1 Modeling of Viscosity Parameters 117
6.4.2 Compositional Property Correlation 132
6.5 Characterization of Oil Color 134

7. Conclusions and Future Work 150

References 155

Vita 164

List of Figures

Figure		Page
4.1	Energy levels of molecules	31
4.2	Transitions between different energy levels	35
4.3	Types of molecular vibrations	40
4.4	Optical diagram of a Fourier transform infrared spectrometer	45
4.5	Behavior of light passing from a denser medium to a rarer medium at various angle of incidence	50
4.6	Schematic of a Fourier transform NMR spectrometer	53
6.1	Schematic of the On-Site Analyzer-Refinery (OSA-R) version	90
6.2	Partial Least Squares model for viscosity at 210 ^{0}F	96
6.3	Partial Least Squares model for viscosity at 100 ^{0}F	97
6.4	Infrared spectra of few of the representative samples obtained by OSA-R analyzer with the optical path-length as 400μ	104
6.5	Infrared spectra of few of the representative samples obtained by OSA-R analyzer with the optical path-length as 100μ	106
6.6	Partial Least Squares model for viscosity at 210 ^{0}F	108
6.7	Partial Least Squares model for viscosity at 100 ^{0}F	109
6.8	Schematic of the Attenuated Total Reflectance (ATR) cell used for sampling	118
6.9	Infrared spectra of few representative sample obtained by the ATR sampling technique	119
6.10	Predictive model for viscosity at 210 ^{0}F	121
6.11	Predictive model for viscosity at 100 ^{0}F	122
6.12	Predictive model for viscosity index	129
6.13	Predictive model for paraffinic composition in the samples	135
6.14	Predictive model for naphthenic composition in the samples	136
6.15	Predictive model for aromatic composition in the samples	137

6.16 Visible spectra of few of the representative samples 145
6.17 Partial Least Squares predictive model for the color of the samples 147
7.1 Schematic of the proposed prototype on-site analyzer 153

List of Tables

Table		Page
1.1	Elemental composition of crude oils	3
1.2	Typical crude oil fractions and their boiling ranges	9
4.1	Spectroscopic characteristics and corresponding regions	33
4.2	Infrared absorption frequencies of few hydrocarbon groups	46
6.1	Description of the Impact 400 FT-IR spectrometer from Nicolet	91
6.2	Physical properties of few representative samples	93
6.3	Prediction of viscosity at 210 ^{0}F	98
6.4	Prediction of viscosity at 100 ^{0}F	101
6.5	Prediction of viscosity at 210 ^{0}F	110
6.6	Prediction of viscosity at 100 ^{0}F	114
6.7	Prediction of viscosity at 210 ^{0}F	123
6.8	Prediction of viscosity at 100 ^{0}F	127
6 9	Prediction of viscosity index	130
6.10	Prediction of relative paraffinic content	138
6.11	Prediction of relative naphthenic content	140
6.12	Prediction of relative aromatic content	142
6.13	Prediction of the color of the sample	148

Chapter 1

Petroleum Chemistry

1.1 Introduction

Petroleum is a term derived from the Latin words *petra* (rock) and *oleum* (oil), which is used to define the wide range of naturally occurring hydrocarbon mixtures. Petroleum includes components that are gaseous, liquid and solid. Commonly all three forms are produced together with gases and solids within a liquid. However, both the solid and the gaseous forms can occur separately. Examples are natural gas and natural asphalt.

Petroleum chemistry is the chemistry of hydrocarbons. The bulk of the compound in the crude oils are hydrocarbons and the remaining compounds, which are as little as 2%, contain other elements, in particular nitrogen, sulfur, and oxygen. Petroleum deposits vary widely in their physical and, to a lesser degree, their chemical properties. Having said that crude oils are predominantly mixtures of hydrocarbons, the question "Why are various crude oils totally different from one another?" may arise. The answer lies in the very wide range of organic compounds, which can be found in the crude oil. The physical and chemical properties of these

crude oils reflect the different proportions of the various compounds, each with its own properties, which go to make the mixtures we call crude oil. Many of the physical properties of hydrocarbons, such as specific gravity, boiling and melting points vary with chain length. In general, the larger the molecule the denser it becomes, and the higher its boiling and melting points. Thus the heavy, viscous oils have a higher proportion of larger molecules as compared with the lighter, less viscous oils. In spite of all these differences in properties, the elemental analysis of crude oil shows that the proportions of the element in the petroleum vary only slightly over narrow limits. Table 1.1 shows the range of elemental composition of crude oils.

1.2 Chemical Composition

The high proportion of carbon and hydrogen indicate that hydrocarbon are the major constituents of petroleum. Elements other than carbon and hydrogen, i.e., nitrogen, oxygen and sulfur appear as organic compounds and while, they occur in relatively small proportion in petroleum, they can, in the heavier asphaltic crude oils, constitute a considerable percentage of the whole.

Table 1.1 Elemental composition of crude oils.
[Source: Robert Richard Francis Kinghorn, "An introduction to the physics and chemistry of petroleum". John Wiley & Sons, 1983.]

Element	Weight Percentage
Carbon	84-87
Hydrogen	11-14
Oxygen	0.1-2.0
Sulfur	0.06-2.0
Nitrogen	0.1-2.0

1.2.1 Hydrocarbon Components

The hydrocarbon components of petroleum are composed of paraffinic, naphthenic and aromatic groups. Olefinic groups are not usually found in crude oils and acetylinic hydrocarbons are very rare indeed. It is convenient to divide the hydrocarbon components of petroleum into three categories: (1) Paraffins, (2) Naphthenes, and (3) Aromatics [2].

1.2.1.1 Paraffins

Paraffins are a homologous series of saturated hydrocarbons of general formula C_nH_{2n+2}. They may have either straight or branched chains, but without any ring structure. The simplest member of this series is methane (CH_4) followed by ethane (C_2H_6) and so on. In crude oils all the normal alkanes from C_1 to C_{40} have been identified.

1.2.1.2 Naphthenes

These are saturated hydrocarbons containing one or more rings, each of which may have one or more paraffinic side chains. The smallest of these

compounds is cyclopropane, which has three carbon atoms. In crude oils the most common naphthenes are the five and six membered rings, and occasionally a few have rings with seven carbon atoms. Crude oil can contain 50% of naphthene compounds, although a majority of these molecules may be in the higher molecular-weight fractions and are the fused-rings naphthenes rather than the simple naphthenes found in the lower-boiling fraction [3].

1.2.1.3 Aromatics

These are hydrocarbons containing one or more aromatic nuclei, such as benzene, naphthalene, and phenanthrene ring systems which may be linked up with naphthene rings and/or paraffinic side chains. Aromatics rarely amount to more than 15% of the total crude oil and they are frequently concentrated in the heavy fractions, e.g. in gas oil, lubricating oil and residuum [1].

1.2.2 Non-hydrocarbon Components

Crude oils contain appreciable amounts of organic non-hydrocarbon constituents, mainly sulfur, nitrogen and oxygen containing compounds and in smaller amounts organometallic compounds in solution and inorganic salts in colloidal suspension. These tend to concentrate mainly in the nonvolatile residues.

Although their concentration in certain fractions may be quite small, their influence is important. For example, the deposition of inorganic salts suspended in the crude can cause serious breakdowns in refinery operations; the thermal decomposition of deposited inorganic chlorides with evolution of free hydrochloric acid can give rise to serious corrosion problems in the distillation equipment. In catalytic operations, passivation and/or poisoning of the catalyst can be caused by deposition of traces of metals (vanadium, nickel) or by chemisorption of nitrogen containing compounds on the catalyst, thus necessitating the frequent regeneration or replacement of catalyst.

1.2.2.1 Sulfur

Sulfur compounds of one type or another is present in all crude oil; in general, the higher the density of the crude oil, the higher the sulfur contents. The total sulfur in the crude can vary from 0.04% for light paraffin oil to 5.0% for a heavy crude oil [3]. Sulfur compounds in petroleum vary from the thiols (R-SH) to the polycyclic sulfides, such as compounds with five and six membered rings.

1.2.2.2 Nitrogen

Nitrogen compounds are undesirable in crude oils. They cause the poisoning of catalysts and the formation of gum in fuel oils. The nitrogen content of petroleum is low and generally falls within the range 0.1 – 0.9%, although crude oils with no detectable nitrogen or even trace amounts are not uncommon. The compounds that have been most investigated are those which can be easily separated and include pyridines, quinolenes, indoles, pyrolles and carbazoles [3].

1.2.2.3 Oxygen

The total oxygen content of petroleum is usually less than 2% although larger amounts have been reported. However, in cases where the oxygen content is phenomenally high it may be that the oil has suffered prolonged exposure to the atmosphere either during or after production. The oxygen content of petroleum does increase with the boiling point of the fraction [3].

1.3 Crude Oil Distillation

In the early stages of petroleum refinery development, when illuminating oil and lubricating oils were the main products, distillation was the major, and often

only, refinery process. As the demand for gasoline increased, conversion processes were developed because distillation could no longer supply the necessary amount.

Refining processes now have a series of steps that eventually converts the crude oil into marketable products. These refining steps vary depending upon the on the crude oil and the products required. The processes have to be selected and products manufactured to give a balanced operation [2].

Distillation has remained a major refinery process. It is a process to which every crude oil entering the refinery is subjected. The most important and primary function of distillation in the refinery process is to separate the crude oil into component fractions. Table 1.2 shows the typical crude oil fractions along with their boiling ranges.

It is possible to obtain products, which range from low-boiling materials to heavy "non-volatile" residue or "bottoms" with lighter materials taken off at intermediate points. The bottoms or heavy fractions of crude require so high temperatures for atmospheric distillation that thermal cracking would occur, with the resultant loss of products and equipment fouling. These materials are therefore distilled under vacuum because the boiling temperature decreases with the lowering of pressure.

Table 1.2 Typical crude oil fractions and their boiling ranges.
[Source: Gary, J.H.; Handwerk, G.E. " Petroleum Refining: Technology and Economics". Marcel Dekker, 1984.]

Fraction	Boiling Ranges (^{0}F)
Butanes and Lighter	
Light straight-run gasoline	90-220
Naphtha (heavy straight-run gasoline)	180-400
Kerosine	330-540
Light gas oil	420-640
Atmospheric gas oil	550-830
Vacuum gas oil	750-1050
Vacuum reduced crude	1000+

Of all the units in refinery, the distillation unit is required to have the greatest flexibility in terms of variable quantity of feedstock and range of product yield. The maximum permissible temperature of the feedstock in the distillation unit is the factor limiting the range of products of products in a single stage atmospheric column and hence, multiple stages are required depending upon the product desired.

1.4 Petroleum Products

In the early days of the oil industry, the simple fractions obtained from distillation were directly used as marketable products. There have been many changes in emphasis on product demand since the inception of the petroleum industry. Nowadays, almost all petroleum products have to be specially tailored, in terms of properties and freedom from impurities, to meet the exacting market demands. Most marketed products are blends sometimes containing as many as six components. The process of blending is simple but determination of how much of each component to include in the blend is a difficult task. In the following section a general overview of some of the petroleum products is presented.

1.4.1 Gas

During the distillation of crude oil, considerable volumes of gas (methane, ethane, propane, and butanes) are released. Further quantities of gases are generated in the various reforming and cracking processes of refinery as a result of the breakdown of heavier fractions. Such gas has higher calorific values than the fuel oil and thus can be used with advantage as a fuel for refinery process units. There are often other demands on refinery gas since the lighter paraffins can be easily converted to "synthesis gas" (carbon monoxide and hydrogen) which is the starting point for the manufacture of many chemical products including ammonia and methanol and their derivatives. Butane is an essential constituent in imparting desirable volatility and anti-knock properties to gasoline. Butanes and butenes can be easily maintained in the liquid state at ambient temperature under quite moderate pressures, and can therefore be marketed in steel containers, which can be safely used in home for heating and cooking.

1.4.2 Gasoline

Gasoline is a complex mixture of hydrocarbons that boils below 200^0C. The hydrocarbon constituent in this boiling range are those that have 4-12 carbon atoms in their molecular structure. Earlier in the century the only source of gasoline was

that which was originally present in the crude oil. Later it was discovered that the heavier portion of the crude oil could be thermally degraded to smaller molecules, which were in the range suitable for gasoline. With the increase in the demand for gasoline, the technology of degradation/cracking of heavy fraction improved and various processes (catalytic cracking, thermal and catalytic reforming, hydrocracking, alkylation and polymerization) were developed to meet the enhanced demand [4]. Because there is a large difference in the composition of the gasolines coming from different processes, gasoline blending is of utmost importance. Blending of up to a dozen hydrocarbon stream may be needed to produce quality gasoline [5]. Also, the introduction of new processes and changes in the specifications of the finished gasoline dictate re-evaluation of the components that make up the gasoline.

1.4.3 Petroleum Solvents

Petroleum solvents have been available since the early days of the petroleum industry and are also referred to as industrial naptha. They are valuable as solvents because of their nonpoisonous character, good dissolving power and inherent stability.

In recent years the range of petroleum solvents has been considerably extended following the development of cracking processes which apart from yielding gasoline fractions also produces important solvents and intermediates which were previously obtained only from coal carbonizing industry. The wide range of napthas now available and the varying degree of volatility possible offer products suitable for many uses. The wide use range is supported by the ready availability in large volume and the low cost relative to the other alternative solvents.

The main uses of petroleum napthas are in deposition industries which includes paints, printing ink and polish manufacturers, the rubber and adhesive industries, extraction industries which deal with the preparation of edible oils, perfumes, glues and fats [5]. Further uses are found in dry-cleaning, leather and fur industry and also in the pesticide field.

1.4.4 Kerosene

In the early stages of petroleum industry, kerosene was its largest and most selling product. Kerosene originated as a distilled petroleum fraction, which boiled between approximately 205 and 260 ^{0}C. The quantity and quality of kerosene vary with the type of crude oil. It is a very stable fraction and does not need any additives for enhancing its properties.

1.4.5 Fuel Oils

Fuel oil if used without further qualification can be interpreted differently. Fuel oil is generally associated with the residual material remaining as a result of refinery distillation of crude oil either alone or in blend with light components. They are often also associated with the middle distillate or gas oils, which are also used as fuels and are distinguished from the residual type fuels by being characterized as distillate fuels.

The terms distillate fuels and residual fuels are now losing their significance, since fuel oils are now made to meet specific requirements and may be either distillate, residual or mixture of both. The terms, domestic fuel oils, diesel fuel oils and heavy fuel oils are more indicative of the uses and composition of the fuel oils.

1.4.6 Lubricating Oil

The major function of lubricating oils is the separation of metal surfaces, which are moving with respect to one another, thereby reducing the friction and wear. Petroleum base lubricating oils are present in the residue boiling above 400 ^{0}C from the atmospheric distillation of crude oils. This residue is further distilled under

conditions of high vacuum into a series of fractions to provide light to heavy lubricating oil stocks. The number of fraction depends upon the type of the crude oil and the requirements of the refiner, but four to five is a typical number [5]. These basic stocks are further processed to get de-asphalted and de-waxed oils suitable for incorporating into finished lubricants. The individual refined stocks are blended in various proportions to provide lubricating oil suitable for a wide range of application. In majority of the cases chemical additives are added to enhance properties of the base oils to meet specific applicational requirements. These additives are used to enhance characteristics as the oxidation resistance, change in viscosity with temperature, low temperature flow properties, anti-wear and frictional properties, corrosion and radiation resistance.

1.4.7 Waxes

Wax, although regarded as an undesirable material when manufacturing lubricating oil, is nevertheless of intrinsic value as separated product. The wax that are removed from light lubricating oil has relatively large crystals, and are referred to as "paraffin wax". Those obtained from the heavier fractions have much smaller crystals and are referred to as "micro-crystalline wax". The latter has higher molecular weights, smaller crystal structures and greater affinity for oil than the paraffin wax. Paraffin waxes also exhibit pronounced latent heats of crystallization.

Wax is one of the most versatile products of the oil industry. They are used as a source of light and heat in applications such as candles, tapers, matches and flares. They provide strength, moisture proofing, appearance and low cost for the food packaging industry. The coating of corrugated board with hot melts is of increasing importance to the wax industry. Wax is also used as feedstock for the production of numerous petrochemicals.

Chapter 2

Petroleum Characterization

2.1 Importance

Crude oil is a complex mixture of hydrocarbons plus organic compounds of sulfur, nitrogen and oxygen. They exhibit wide variations in compositional and physical properties, and these occur not only in crudes from different fields but also in oils taken from different production depths in the same well. The physical and compositional properties of a crude oil play a large part not only in determining the nature of the products that arise from the refining operations but also in determining the means by which particular crude should be processed [2].

The refinery products have to be often blended before they can be marketed as a marketable product. The physical blending requires thorough knowledge of the product characteristics. Each refinery product has a different physical and compositional properties and hence, the selection of the components and their proportions in the blend is one of the most complex problems in the refinery.

At the present time, the pressure of competition, the technological advances and the need for the products with better quality has put a great emphasis on the process and quality control in the refineries. This requires a fast and accurate method for the characterization of the products.

In the recent years the stringent environmental requirements and depleting oil fields poses new problem to the petroleum industry. The industry faces the challenge of developing new processes to upgrade the petroleum residues, oil sands and oil shale bitumen to valuable light oils. This requires easy and reliable techniques to follow changes in composition at various stages of transformation and to control the quality of the products finally obtained.

The importance of the physical and compositional characterization of crude oil and its products cannot be overstressed. At this point the question arises as to what are the principal physical and compositional properties that needs to be specified so as to give adequate process monitoring and quality control in the refinery. The following section would provide the answers to these questions.

2.2 Important Oil Characteristics

As mentioned in previous chapter, each refinery product has varying physical and compositional properties. The products have different use in the market and hence, have to meet different specifications. Thus, a universal set of properties cannot be used to establish the characteristics/specifications of the numerous refinery products.

For example, the primary requirement of a gasoline fraction is that its combustion should be smooth, starting at the spark plug and spreading evenly through the chamber. It should not readily cause detonation or knocking in the engine. On the other hand, the major function of lube oil fraction is to reduce friction and wear in the moving parts of a machine. Therefore the quality criteria applicable for lube oils are quite different from those of gasoline; while "Octane number" is an important specification in gasoline characterization, it holds no meaning as far as lube oils are concerned.

The discussion of all such specifications is beyond the scope of the thesis. However, there are some properties that are important to all petroleum products and are discussed in the following section. Various standard organization such as the American Society for Testing and Materials (ASTM) in North America and the

Institute of Petroleum (IP) in Britain have standardized the methods for the evaluation of petroleum properties. A brief mention of the standard method of evaluation of these properties has been included and for convenience, reference has been made to the corresponding ASTM test.

2.2.1 Composition

All physical properties of oils are dependent upon the composition of the oils and hence, the compositional characterization of the oils is of great importance. Composition of oil can be specified in a number of ways. It can be reported in terms of the total carbon and hydrogen contents or in terms of the major hydrocarbon type constituents; paraffins, naphthenes and aromatics (PNA).

The standard ASTM method for carbon and hydrogen content is the classical combustion technique, ASTM D5291. For the PNA analysis, the standard method is the fluorescent indicator adsorption (FIA) technique.

2.2.2 Specific Gravity

In the early years of petroleum industry, specific gravity was the principal specification for crude oil and its products. They are used for characterizing

unknown oils since they correlate approximately with the hydrocarbon composition and, therefore, with the nature of the crude source of the oil. The hydrometer method is used for evaluating the specific gravity of the oil (ASTM D1298).

2.2.3 Viscosity

The viscosity is the measure of the flow characteristics of the fluid. This is measured by timing the flow of a fixed amount of oil through a calibrated glass capillary tube under gravitational force at a standard temperature, and is known as the kinematic viscosity of the oil (ASTM D445). The unit of viscosity used in this method is centiStoke, but this may be converted to other viscosity systems such as Saybolt Second Unit (ssu), Redwood, and Engler by means of tables.

Viscosity is an important property especially for fuel oils and other heavier fraction. It is used to identify grades of oil and for following the changes caused in the oil in service. Viscosity of diesel fuels and gasoline is important primarily because of its effect on the handling of the fuel by the pump and injector system.

2.2.4 Viscosity Index

The viscosity of petroleum and its product varies with temperature. The rate of variation with temperature depends upon the composition of the material. The viscosity index is an empirical number, which indicates the effect of change of temperature on the viscosity of the oil. A high viscosity index denotes a low rate of change of viscosity with temperature and vice versa. Products with high paraffinic content have high viscosity index, while those with high naphthenic/aromatic content have low viscosity index. ASTM method D2270 is used to specify the viscosity index of the oils.

Viscosity index of oil is an important parameter in applications where an appreciable change of temperature is expected. One such application is the lubricating oils used in automatic transmissions.

2.2.5 Flash Point

This gives the indication of the presence of volatile components in oil. It is the temperature to which oil must be heated under specified test conditions to give off sufficient vapor to form a flammable mixture with air. The Cleveland open cup method (ASTM D92) is used to determine the flash point of oil.

From the viewpoint of safety, flash point is one of the most important parameter especially in cases where high temperature operations are encountered. In the case of used oils, the flash point is used to indicate the extent of contamination with a more volatile oil or with fuels. Flash point can also be used to assist in the identification of different types of product blend.

2.2.6 Color

The color of oil and its products is measured in a standard glass container by comparing the color of the transmitted light with that transmitted by a series of numbered glass standards, and the best match is noted (ASTM D1500).

Color is used for manufacturing control purposes, and is important since the consumer readily observes it. Where the color range of a particular product is known, a variation outside the established range indicates possible contamination with another product. However, since the standard measurement technique for color is so subjective, it is not indiscriminately used for product specifications.

2.3 Overview of Characterization Techniques for Petroleum

In this section a brief overview of the techniques used for characterizing petroleum and its products is presented. The standard techniques for characterizing petroleum have been formalized by ASTM. Most routine evaluations in petroleum analytical labs are performed using test methods established by ASTM or other such standard organizations. Apart from the ASTM methods, many other techniques are prevalent in the industries and their results often confirm with those obtained from the standard tests. These alternative methods are based mostly on spectrometric techniques like Fourier Transform Infrared (FTIR) spectroscopy, Ultraviolet (UV) spectroscopy, Nuclear Magnetic Resonance (NMR) spectroscopy, Gas Chromatography (GC), High Performance Liquid Chromatography (HPLC) and Raman spectroscopy.

Study has shown that mid-band FTIR combined with multivariate calibration analysis is a versatile, efficient and accurate method for the simultaneous measurement of key gasoline properties within 1 min with less than 2 ml of sample. The FTIR derived properties include octane number, aromatic and saturated hydrocarbon content and concentration of ethanol and methyl tert-butyl ether. This new methodology could increase the corresponding output of the petroleum laboratories by a factor of over 200 to 1 while maintaining data integrity and

minimizing sample requirements, environmental hazards and cost [6]. On the other hand, conventional method for octane number by ASTM knock engine method is time consuming and cumbersome.

Although the FIA method is being used as the official method in the petroleum industry for the estimation of PNA content in the oils, it has significant shortcoming [7]. The method does not give carbon number distribution or individual component identification [8]. Multicolumn Gas Chromatography (MC-GC) has advantages over the existing FIA method. They require no initial sample preparation, a single chromatographic run completes the whole analysis, the results have excellent precision as compared with ASTM FIA method and it requires considerably less time [8].

A group property approach has been developed to predict 17 physical properties of middle distillate from experimentally derived liquid chromatography/proton NMR data. Some of the physical properties that have been obtained by this technique include cetane number, cetane index, density, specific gravity, flash point and viscosity. The predictions of these properties fall within the ASTM method reproducibility for the measurement of the listed properties and at the same time requires less analysis time and sample volume than the corresponding ASTM methods [9].

Though the standard ASTM methods may be accurate and enjoy a high degree of acceptance, they also have some disadvantages. They require large sample sizes, they may be cumbersome, they may use toxic or environmentally dangerous chemicals and they are time and labor intensive [10]. On the other hand, spectrometric techniques are fast, reliable and require minimal labor. These inherent advantages of spectrometric methods have helped in popularizing these techniques in the petroleum industry.

Chapter 3

Research Objective

The broad objective of this research is to develop optical spectrometric techniques (FTIR, UV/visible spectroscopy) for characterizing heavy oil fraction in the petroleum industry. The ultimate aim was to incorporate the techniques developed in this research into a prototype instrument that could be used for either on-line or off-line characterization of the heavy oil fractions.

A variety of standard characterization techniques for heavy oil fractions exist in the industry. However, they have inherent drawbacks that have been discussed in the section 2.3. The optical spectrometric characterization techniques developed in this research were aimed at overcoming the drawbacks present in the existing standard characterization procedures. The intention was to develop characterization techniques that were rapid so that the results from it could be effectively used for process and quality control. The spectrometric techniques utilized in this research were Fourier Transform Infrared (FTIR) spectroscopy, visible spectroscopy and Nuclear Magnetic Resonance (NMR) spectroscopy.

The properties characterized in this work are, physical characteristics, compositional characteristics, and optical characteristics.

Physical Properties: The physical properties that are characterized are, viscosity at 100 and 210 ^{0}F (V_{100} and V_{210}) and the Viscosity Index (VI) of the heavy oil fraction.

Compositional Properties: The relative percentage of Paraffin, Naphthene and Aromatics (PNA) present in the heavy fractions.

Optical Property: The color of the heavy oil fractions is characterized in this work.

The infrared spectrum is a unique physical property of the oil under study and differs from other physical properties such as, viscosity, VI, flashpoint, etc., because it is not a single parameter determination [11]. It in fact contains a wealth of information that reflects the physical and chemical properties of the oil samples. In the present work, this characteristic of the infrared spectrum has been utilized to correlate the infrared spectrum of the oil samples to its physical and compositional properties.

The color of the heavy oil fractions can be attributed to the aromatics present in the sample. The concentrations of these types of chemical moeties in the samples are below the detection level of infrared and hence, cannot be used for characterization purpose. The visible spectra of the samples were used to do the color characterization of the samples.

NMR was used to establish the standard composition of the oil samples in terms of percentage PNA. Then the infrared spectrum was correlated to compositional properties determined by the analysis of NMR spectra.

For quantitative correlation, multivariate statistical analysis was used. The software routines in the chemometric toolbox of MATLAB environment were used in the present work. Routines for statistical analysis that were not offered by the chemometric toolbox were developed in C on HP unix platform. The Graphical User Interface (GUI) for these customized routines was developed using visual basic.

Chapter 4

Overview of the Spectroscopic and Quantitative Techniques

This chapter reviews the spectroscopic and the quantitative techniques used in the research work. The basics of electronic, vibrational and magnetic resonance are discussed. Fundamentals have also been included of Partial Least Sqaures (PLS) modeling and clustering analysis such as Principal Component Analysis (PCA).

4.1 Principles of Electronic Spectroscopy

Spectrum of a molecule reflects the change in its energy state. The energy of a molecule can be separated into three additive components associated with (1) the motion of the electrons in the molecules, (2) the vibrations of the constituent atoms, and (3) the rotation of the molecule as a whole. These three components of the energy states of a molecule are shown in Figure 4.1. As evident from this figure, rotational intervals tend to increase as the rotational quantum number J' increases. The vibrational intervals decrease as the vibrational quantum number v' increases. Based on the differences in the energy levels of a molecule, electronic, vibrational and pure rotational spectra are usually observed in the visible and ultraviolet,

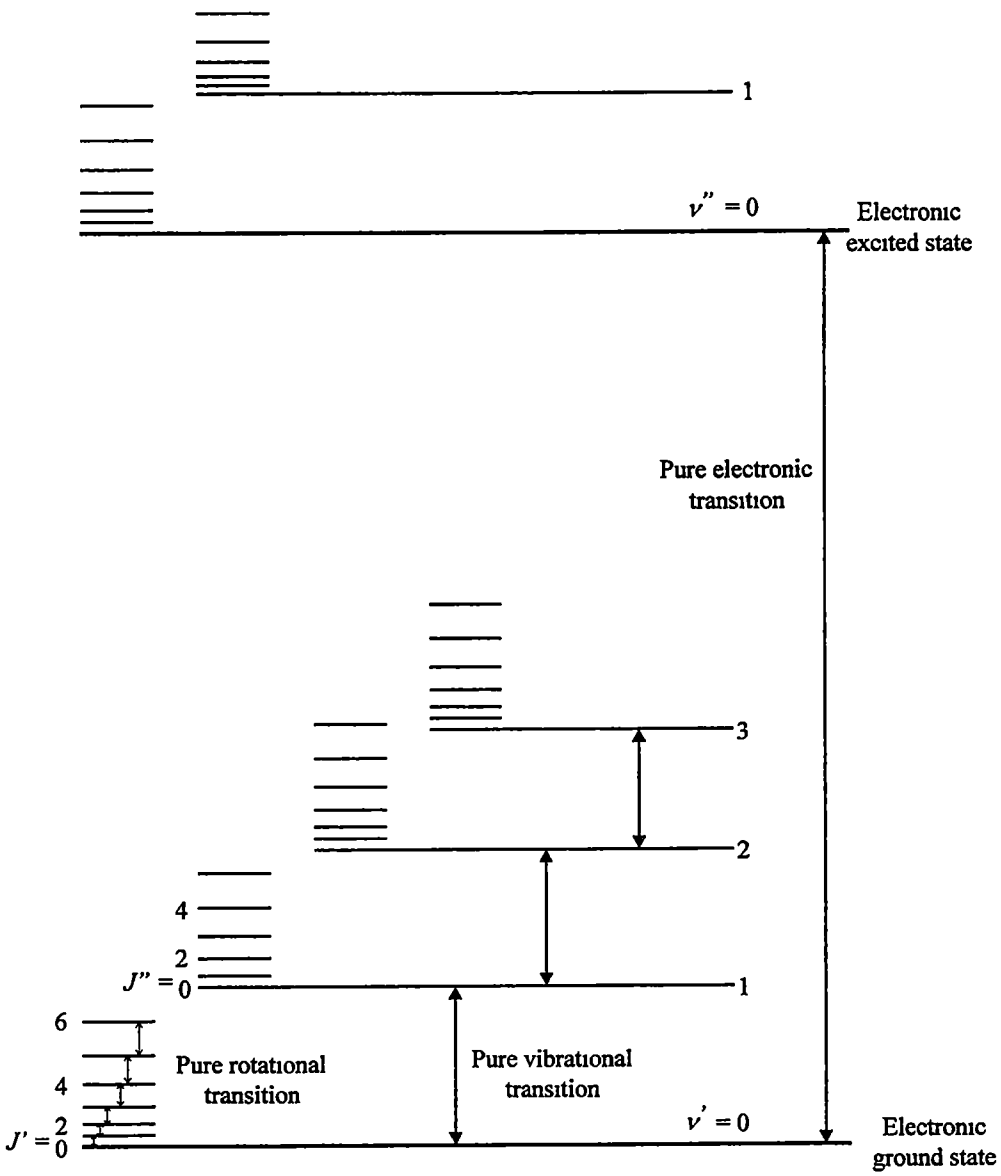


Figure 4.1 Energy levels of molecules
[Source: K. Nakamoto, "Infrared and Raman Spectra of Inorganic and Coordination Compounds". John Wiley & Sons, 1986.]

infrared, and microwave regions respectively. The range of energy, in wavenumber, associated with each of these transitions is listed in Table 4.1.

4.1.1 Origin of Electronic Spectroscopy

Electronic spectrum arises due to transition of the electrons between molecular orbitals. The energy difference between molecular orbitals in organic and inorganic molecules normally lies between 1.5×10^5 to 6×10^5 $J.mol^{-1}$, and the corresponding transition gives rise to absorption in the ultraviolet and visible region of the spectrum [12].

Molecular orbital is described as a linear combination of atomic orbitals. When two atoms forms covalent bonds, then the atomic orbitals of those atoms combines to form two new orbitals; bonding and anti-bonding molecular orbital. The bonding orbital has a lower energy level as compared to the anti-bonding orbital. Therefore the electrons in the absence of any excitation resides in the bonding orbital.

There are two possible linear combinations of the atomic orbitals that can occur during the bonding. They are as follows: (1) two *s* orbitals or two *p* orbitals can overlap head-to-head to form two σ orbitals (σ being the bonding orbital and σ^*

Table 4.1 Spectroscopic characteristics and corresponding regions.

Region	Wavelength (nm)	Characteristic Measured
Ultraviolet (UV)	190-360	Transitions of delocalized π electrons
Visible (Vis)	360-780	Electronic transitions: color measurements
Near Infrared (NIR)	480-2,500	Overtone and combination bands of fundamental molecular vibrations
Middle Infrared (MIR)	2,500-25,000	Fundamental molecular vibration: stretching, bending, wagging, and scissoring
Far Infrared (FIR)	25,000 to 10^6	Molecular rotation

being the anti-bonding), and (2) two p orbitals can overlap in a parallel manner to form two π orbitals (π being bonding and π^* being anti-bonding). The π orbital only exists in double or triple bonds, and their charge distribution is characterized by a nodal plane, the region of low charge density, along the axis of the bond and a maximum density in regions above and below the plane [12].

The relative energy positions corresponding to the different types of molecular orbital are shown in Figure 4.2. Vertical lines in the figure represent the possible electronic transitions among these orbitals. The energy of a non-bonding orbital is generally greater than the σ and π orbital but lower than the σ^* and π^* orbitals. However, in molecules having high degree of conjugation, the energy of π orbitals is greater than the n orbitals. In such cases, less energy is required to promote a π to π^* transition than to promote an n to π^* transition and the absorption band corresponding to the π to π^* transition will occur at longer wavelength than that for the n to π^* transition [12]. Ultraviolet or visible radiation generally results from excitation of bonding electrons. As a consequence, the wavelengths of absorption peaks can be correlated with the types of bonds that exist in the species under study. Molecular absorption spectroscopy is therefore valuable for identifying functional groups in a molecule for the quantitative determination of compounds containing absorbing groups.

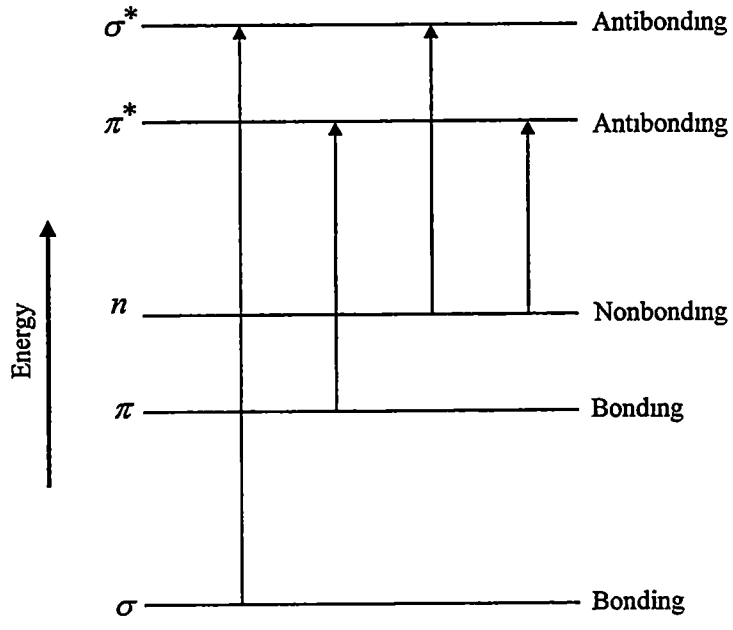


Figure 4.2 Transitions between different energy levels

[Source: B .G. Wells, "Introduction to Molecular Theory and Experiments". Academic Press 1970.]

4.1.2 Features of Electronic Transitions

There are four possible electronic transitions in a molecule (Figure 4.2). They are as follows:

(1) n to π^* Transition

Unsaturated molecules that contain atoms such as oxygen, nitrogen, and sulfur often show a weak absorption band in their spectrum that can be assigned to the n to π^* transition. These transitions can be considered to involve the excitation of an electron in a non-bonding atomic orbital, i.e., unshared electrons on O, N, S, or halogen atom, to an anti-bonding π^* orbital associated with an unsaturated center in the molecule. For example, in saturated ketones and aldehydes, the bands due to n to π^* transition generally occurs in the range 200-250 nm [12].

(2) σ to σ^* Transition

This is the only transition that is possible in a saturated hydrocarbon. The energy required for such transitions is large. This type of transition lies in the vacuum ultraviolet region of the spectrum. Since, commercial spectrophotometer does not operate below 180 nm, the whole of the σ to σ^* transitions cannot be normally observed.

(3) n to π^* transition

This transition occurs in compounds containing atoms with lone pair of electrons. The energy required for this transition is less than that required for π to π^* transition. The wavelength of the peak maximum in the n to π^* band of compounds such as ammonia, alkylhalides, aliphatic alcohol, and aliphatic amines, is less than 200 nm. However, due to their broad bands they start to absorb at 260 nm [12].

(4) π to π^* Transition

This kind of transition can occur in any molecules containing π electrons, such as double bond or triple bond or aromatic ring. This transition falls in the wavelength range 200-750 nm and has a strong absorptivity [12].

4.2 Principles of Vibrational Spectroscopy

The vibrational spectrum of a molecule lies in the infrared region of the electromagnetic spectrum. No two substances that absorb in infrared radiation absorb it at the same frequencies and to the same extent. Thus, an infrared absorption spectrum of a substance is as unique as the fingerprint of human. The only exception is that two optical isomer would have the same infrared signature [11]. Moreover, the infrared spectrum of a mixture of components is simply the superposition of the

individual components comprising the mixture, barring those cases where there are hydrogen bonding. This fact is quite in contrast to ultraviolet and visible spectroscopy where pH and other effects negate the additivity [12]. The above properties of infrared spectroscopy make it one of the most important characterization techniques especially in cases where the sample consists of complex mixture of substance.

4.2.1 Nature and Origin of Infrared Spectrum

All molecules that undergo a net change in dipole moment as a consequence of its vibrational or rotational motion absorb infrared radiation. As a consequence homonuclear molecules like O_2, N_2, Cl_2 etc. does not absorb infrared radiation. Similarly ionic materials like NaCl, KBr, etc. do not have a changing dipole moment and hence, does not absorb infrared radiation. Prisms made from such ionic material are used for dispersing infrared radiation since they act as an excellent window for infrared rays.

Molecules exhibit two basic vibrations: (1) stretching, and (2) bending. A stretching vibration involves a continuous change in the interatomic distance along the axis of the bond between two atoms. Bending vibrations are characterized by a change in the angle between two bonds and can be classified as scissoring, rocking,

wagging, and twisting. The various types of bending vibration are shown schematically in Figure 4.3.

4.2.2 Quantum Treatment of Vibrations

For diatomic molecules, molecular vibration can be approximately treated as a harmonic oscillator. Through quantum mechanical consideration, the vibrations of two nuclei in a diatomic molecule can be reduced to the motion of a single particle of mass μ, whose displacement from its equilibrium position is equal to the change of the internuclear distance. Reduced mass, μ, can be written in terms of the individual masses of the molecules, m_1 and m_2, as follows:

$$\mu = \frac{m_1 m_2}{m_1 + m_2} \tag{4.1}$$

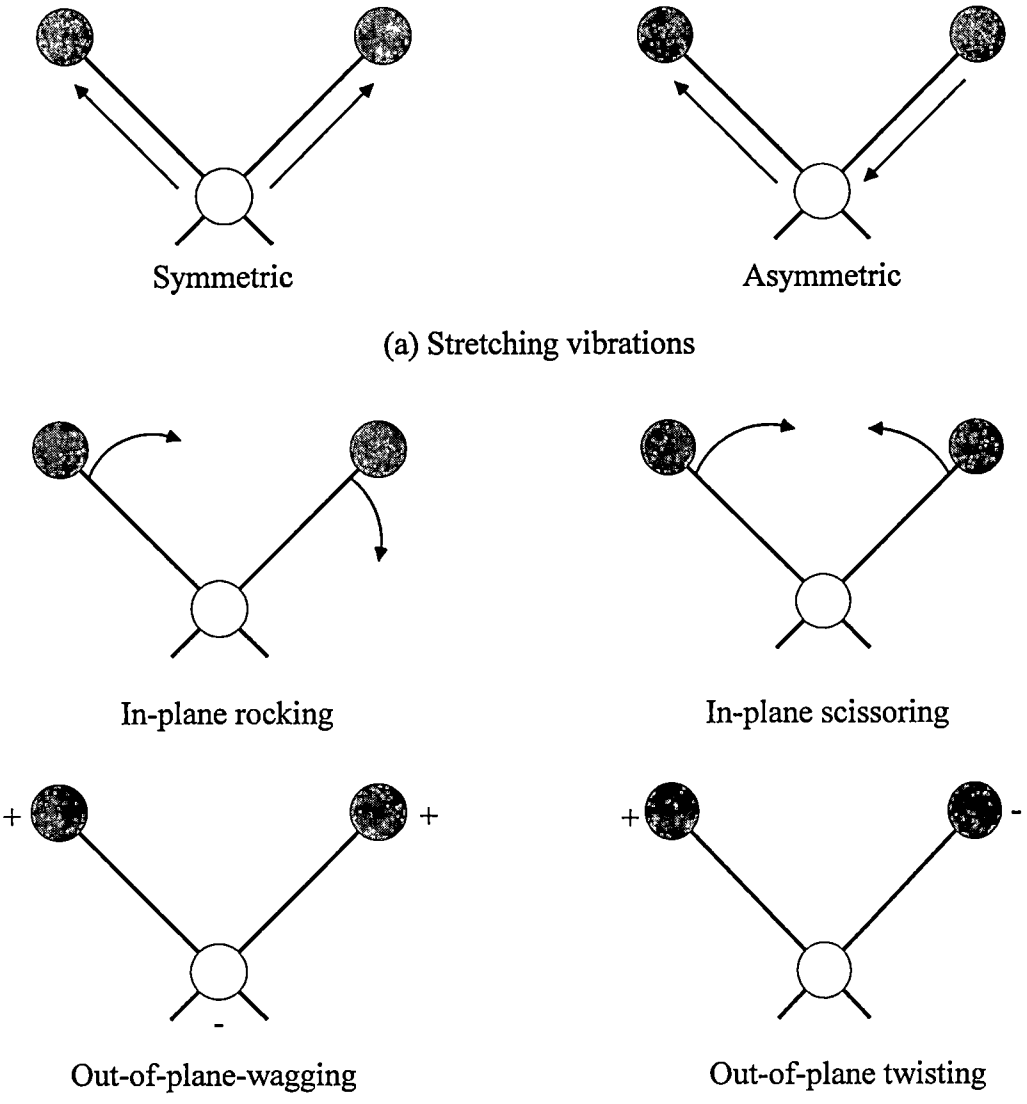


Figure 4.3. Types of molecular vibrations.

Note: + indicates motion from the page toward the reader;

- indicates motion away from the reader)

[Source. D. A. Skoog and J. J. Leary, "Principles of Instrumental Analysis".Saunders College Publishing, 1985.]

The frequency at which the dipole (or ideal harmonic oscillator) vibrates is dependent on the bond strength and the masses of the atoms bonded together. The frequency of the vibration (ν) is given by the relationship [13]:

$$\nu = \left(k/\mu\right)^{1/2}\left(1/2\pi\right) \tag{4.2}$$

where k is the force constant dependent upon the bond strength involved in the vibration. This means that for bonds with similar strength, the bond consisting of heavier atoms has higher vibration frequency. The quantized vibrational energy levels are then determined by

$$E_n = \left[\left(\nu'+0.5\right)h\left(k/\mu\right)^{1/2}\right]\left[2\pi\right]^{-1} \tag{4.3}$$

where E_n = energy value of a discrete quantum number

ν' = the vibrational quantum number

h = Planck's constant

According to the selection rule for the harmonic oscillator, only transitions corresponding to $\Delta v' = \pm 1$ are allowed. Thus, the energy difference between two successive energy levels is:

$$\Delta E = E_{v'} - E_{v'-1} = h\nu \tag{4.4}$$

However, vibrations in the real molecules are anharmonic. Anharmonicity in molecules are due to two reasons: (1) mechanical anharmonicity, and (2) electrical anharmonicity. Mechanical anharmonicity arises if the potential energy as a function of displacement has terms higher than the second degree. Electrical anharmonicity arises if the dipole moment of the vibration is nonlinearly related to the displacement of the vibration. The actual behavior can be mathematically modeled by adding some higher degree terms to the expression in equation (4.3) [13]. Then, we get:

$$E_n = \left(v' + 1/2\right)h\nu - \left(v' + 1/2\right)^2 h\nu x_1 + \left(v' + 1/2\right)^3 h\nu x_2 + \ldots\ldots \tag{4.5}$$

where x_i are the anharmonicity factors.

The application of the anharmonic molecular vibrations can explain the possibility of transitions between two or more than two energy levels. If only the first two terms in equation (4.5) are considered, the energy difference between the first

two successive energy levels in an inharmonic oscillator is given by the following equation:

$$\Delta E = E_n - E_{n-1} = (1 - 2\nu' x_1)h\nu \qquad (4.6)$$

Therefore, the anharmonicity of molecular vibration makes the frequencies of the overtone bands not exactly integral multiples of the fundamental band frequency, and frequencies of combination bands not exactly the summation of frequencies of vibration involved in the combination.

Due to this anharmonicity three kinds of absorption bands can be observed: (1) fundamental bands arising from fundamental transitions (ν' 0 to 1), (2) overtone bands arising from transition (ν' 0 to i, i>1), and (3) combination bands due to simultaneous excitation of two or more vibrational modes. Fundamental bands occur in the middle-infrared (MIR) region, overtone and combination bands in the near-infrared (NIR) region because of the larger excitation energy required.

4.2.3 Spectral Assignment in Infrared

The work presented in this thesis mostly deals with the hydrocarbon compounds found in the heavy fraction of oil. Table 4.2 gives the infrared absorption frequencies of some of the important groups related to the present work.

4.2.4 Sampling Techniques in Infrared Spectroscopy

There are numerous sampling techniques that can be used for infrared spectroscopy. The methods that have been used in this work have been described below. Figure 4.4 illustrates the schematic of a modern FTIR instrument [13]. A manual of recommended practice for the various sampling techniques is available from the ASTM [14]. Two techniques were used in this work: (1) transmission spectroscopy, and (2) Attenuated Total Reflectance (ATR) spectroscopy.

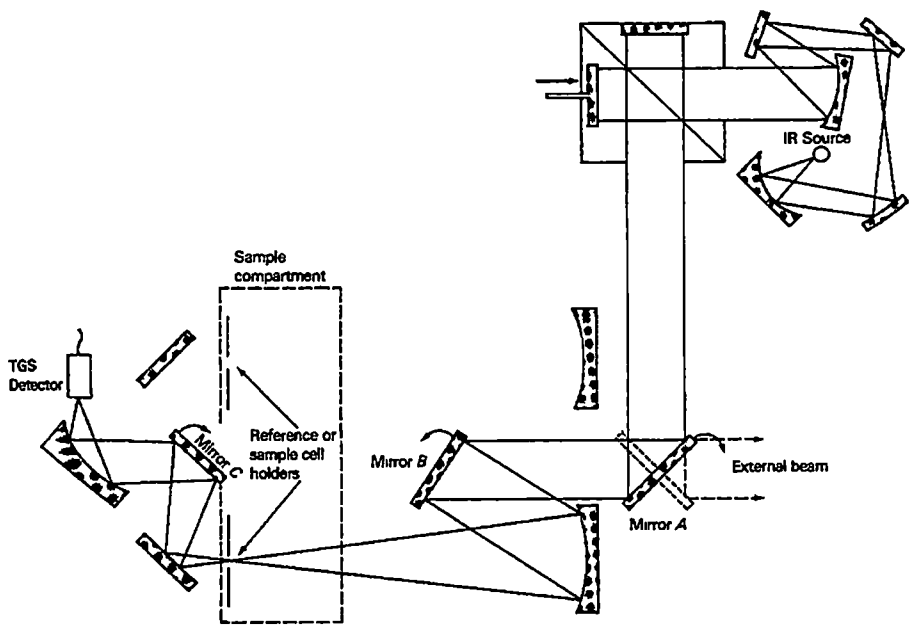


Figure 4.4 Optical diagram of a Fourier transform infrared spectrometer. [Source: D.A. Skoog, " Principles of Instrumental Analysis". Saunders College Publishing, 1985]

Table 4.2 Infrared absorption frequencies of few hydrocarbon groups.

[Source: Smith, A.L. " Applied Infrared Spectroscopy: Fundamentals, Techniques, and Problem-solving". John Wiley & Sons, 1979.]

Group	Compound	Region (cm^{-1})	Remarks
Saturated Aliphatic			
CH_3	RCH_3	2952-2972	Asymmetrical stretching
		2862-2882	Symmetrical stretching
		1450-1475	Asymmetrical deformation
		1377-1383	Symmetrical deformation
	$RCH(CH_3)_2$	~1385	Symmetrical deformation
	$RC(CH_3)_2R'$	1151-1159	Symmetrical deformation
	$RC(CH_3)_3$	~1370	Symmetrical deformation
CH_2	RCH_2R'	2916-2936	Asymmetrical stretching
		2843-2863	Symmetrical stretching
		1450-1475	Symmetrical deformation
	$R(CH_2)_{n>3}$	772-730	Rocking
CH	R_3CH	2890	
		1340	

Table 4.2 continued.

Group	Compound	Region (cm^{-1})	Remarks
Aromatic			
CH		3010-3110	Stretching
		1660-2000	Stretching
CC		1600	Ring mode stretching
	di-substituted	740-830	
	tri-substituted	700-850	
	tetra-substituted	~865	
Ketones		1705-1725	Stretching of carbonyl

4.2.4.1 Transmission Spectroscopy

This mode is used for liquid samples. The transmittance is calculated from the intensity of light passing with (I) and without (I_0) the sample in the path of the infrared beam. The transmittance, T is defined as:

$$T = \left(I / I_0 \right) \times 100\% \tag{4.7}$$

The transmittance is related to absorbance A, by the following equation:

$$A = \log_{10}\left(I_0 / I \right) = \log_{10}\left(1 / T \right) \tag{4.8}$$

Percent transmission is useful for physical measurements, such as characterization of the light absorption of optical filters, while absorbance is mostly used for chemical analysis. The absorbance at a specific wavelength is related to the Beer-Lambert law [13]:

$$A = alc \tag{4.9}$$

where a = absorptivity at a particular wavelength

l = pathlength of the sample

c = concentration of the absorbing species

In the transmission mode, the sample solution is filled in a cuvette/cell and the transmission is recorded. The thickness of the cell is influenced by the concentration of the species of interest in the sample. For trace analysis, cells with pathlength up to 5 cm are used. Where the concentration of the species are high, extremely thin cells (< 0.05 mm) are used. However, very thin cells are difficult to construct, fill and empty and may produce diffraction fringe pattern in the spectrum.

4.2.4.2 Attenuated Total Reflectance

When a beam of light passes from a denser medium to a rarer one, then at a certain critical angle, θ_c, all the incident light is totally reflected back to the denser medium (Figure 4.5). This phenomenon is called *total internal reflection.* ATR spectroscopy is based on the fact that although total internal reflection occurs at the interface of a denser and rarer medium, radiation does in fact penetrate a short distance in the rarer medium. This penetrating radiation, called the *evanescent wave*, can be partially absorbed by placing a sample in optical contact with the denser medium (called prism in ATR spectroscopy). The totally reflected ray then yield an

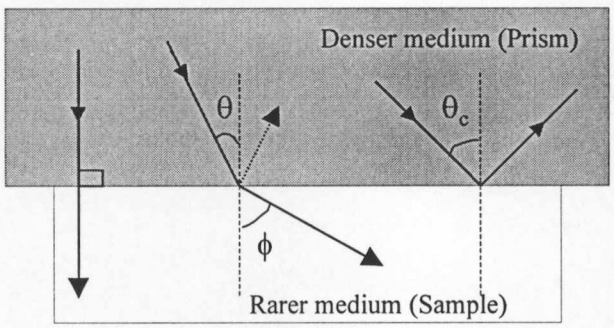


Figure 4.5 Behavior of light passing from a denser medium to a rarer medium at various angle of incidence. When the light ray is incident at the critical angle, θ_c, all of it is reflected to the denser medium.

absorption spectrum that resembles the transmission spectrum. The absorbance values for ATR spectrum is much lower than the transmission spectrum, of the order of the wavelength of the light. However, by producing multiple reflections the absorptivity of the ATR spectroscopy can be enhanced. Another characteristic of the ATR spectroscopy is that the depth of penetration of the evanescent wave is a function of the wavelength of the light. The penetration depth is given by the equation:

$$d_p = \frac{\lambda}{2\pi(\sin^2\theta - n_{sp})^{1/2}} \qquad (4.10)$$

where d_p = depth of penetration

λ = wavelength of the radiation in the prism medium (not in vacuum)

θ = angle of incidence of the beam on the prism sample interface

n_{sp} = ratio of the refractive index of sample to the prism medium

The above equation suggests that longer the wavelength, the more is the penetration. This means that ATR spectrum at longer wavelengths is enhanced as compared to those at shorter wavelength. This is in contrast to transmission spectroscopy where the pathlength of the incident beam is independent of the wavelengths.

4.3 Nuclear Magnetic Resonance (NMR) Spectroscopy

NMR spectroscopy is based upon the measurement of electromagnetic radiation in the radio frequency region of roughly 4 to 600 MHz. This corresponds to the wavelength range of 75 to 0.5 m. In contrast to UV, visible, and infrared absorption, nuclei of atoms rather than the electrons are involved in the absorption process. Figure 4.6 shows the schematic of a modern NMR instrument.

4.3.1 Theory of NMR

The nuclei of an atom rotate about their axis. The angular momentum associated with this spin is an integral or half integral of $h/2\pi$, where h is the Planck's constant. The maximum spin component for a particular nucleus is its spin quantum number I. A nucleus has $(2I+1)$ discrete states of angular momentum. The component of the angular momentum for these states in any chosen direction will have values of I, I-1, I-2... -I. In the absence of any external fields all these states have identical energy.

Since a nucleus bears a charge, its spin gives rise to a magnetic field that is analogous to the field produced when electricity flows through a coil of wire. The

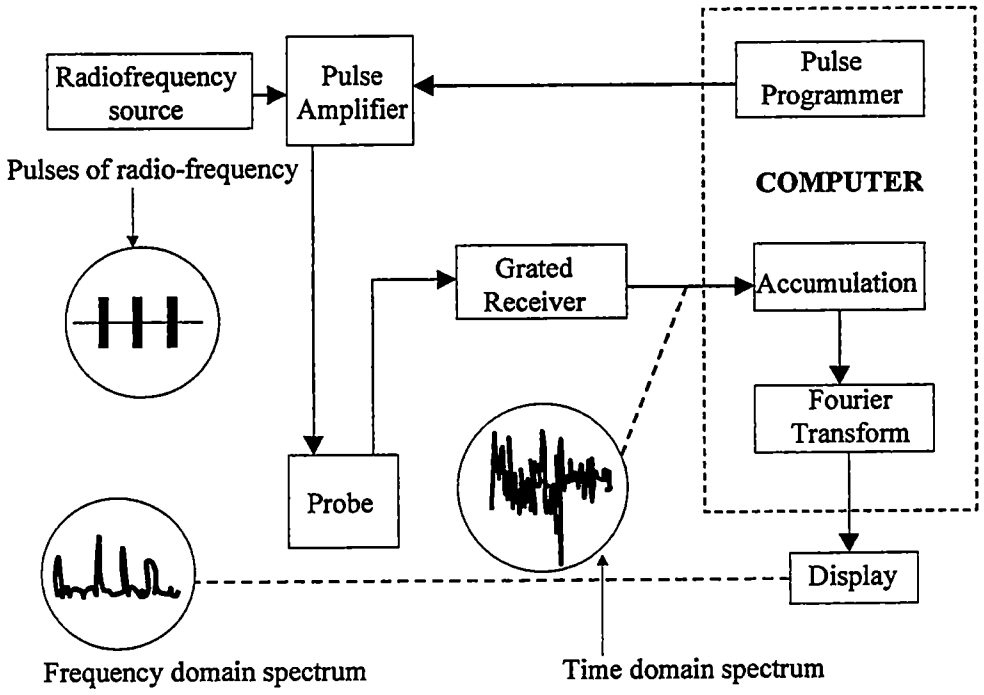


Figure 4.6 Schematic of a Fourier transform NMR spectrometer.

resulting magnetic dipole μ is oriented along the axis of spin and has a value that is characteristic for each type of nucleus. The interrelationship between particle spin and magnetic moment leads to a set of observable magnetic quantum states m, given by:

$$M = I, I-1, I-2, \ldots\ldots, -I \tag{4.11}$$

When brought in an external magnetic field, a particle possessing a magnetic moment tends to become oriented such that its magnetic dipole and hence its spin axis, is parallel to the external field. The potential energy of the dipole depends upon the orientation of the dipole in the field. Since the orientation of the magnetic moment of a nucleus is limited to $(2I+1)$ discrete values, its potential energy in an external magnetic field is also discrete and is given by:

$$E = -\frac{m\mu}{I}\beta H_0 \tag{4.12}$$

where H_0 is the strength of the external magnetic field in gauss (G) and β is a constant called the nuclear magneton (5.051×10^{-24} erg.G^{-1}); and m is the magnetic moment of the nucleus expressed in the units of nuclear magnetons.

The energy difference between each discrete level is given by:

$$\Delta E = \mu\beta \frac{H_0}{I} \tag{4.13}$$

The nucleus can absorb photon with energy that just equals to ΔE to bring about the excitation to a higher nuclear magnetic quantum level. This forms the basis of NMR spectra.

The frequency of radiation absorbed by a nucleus is strongly affected by the kind of chemical environment in which it exists. This variation in frequency is called *chemical shift*. As a consequence, even for a simple molecule, a wealth of spectral detail is observed. The chemical shift arises from the circulation of the electrons surrounding the nucleus under the influence of a magnetic field. This movement of electrons creates a small magnetic field that opposes the external field. Thus, the nucleus is exposed to an effective magnetic field that is somewhat smaller than the external field. This phenomenon depends upon the density of electron surrounding the nucleus, which in turn depends upon the structure of the compound containing the nucleus. Thus the NMR spectra of two different compounds is not similar though they may have the same nuclei in them.

4.4 Quantitative Techniques

The success of any analytical technique lies in the ease and accuracy with which quantitative and qualitative information can be extracted from it. The advancement of computational capabilities in the recent years and the introduction and development of chemometric evaluation procedures for analysis has revolutionized the art of data analysis.

Bebe et.al [15] defines chemometrics as the "science involving the use of mathematics and statistics on chemical data". The purpose of chemometrics is to develop correlation between experimental data (e.g. IR absorption, UV/visible spectra) and the properties of interest (e.g. viscosity of the material, viscosity index, composition of the material, etc.).

The spectra of the heavy fraction petroleum products are very complex. A single wavelength or a few wavelengths are not sufficient to calibrate the properties of interest that were mentioned in the previous chapter. Several wavelengths in the spectra are required to give complete information about the property being calibrated. Therefore, multivariate calibration techniques are required for the analysis. Because of the inclusion of a large number of wavelengths in the calibration model, the use of conventional Multiple Linear Regression (MLR)

techniques for calibration is numerically sensitive to small errors in the data. However, it is noted that the data represented by these wavelengths are highly inter-correlated, and the essential information is contained in only a few variables. Some multivariate techniques involve data reduction of these highly correlated spectra into few factors. These factors explain much of the variance in the data. Partial Least Squares (PLS) and Partial Component Analysis (PCA) are the factor analysis techniques that were used in the present work.

4.4.1 Exploratory Data Analysis-Principal Component Analysis

Principal Components Analysis (PCA) is a favorite way of chemometrican for data compression and information extraction [16,17]. PCA finds combinations of variables or factors that describe major trends in a data set. Thus, a few variables that account for inter-correlations in the original variables are used. This avoids the use of redundant information in the calculations [16,17]. This kind of analysis is called factor analysis and also provides insight into the relationship among the samples and the variables.

In PCA, a spectra matrix **X** ($m \times n$) for m samples at n wavelengths (usually $m < n$) can be mathematically expressed as a product of two matrices as follows.

$$\mathbf{X} = \mathbf{t}_1\mathbf{p}_1^T + \mathbf{t}_2\mathbf{p}_2^T + \ldots + \mathbf{t}_f\mathbf{p}_f^T + \ldots + \mathbf{t}_q\mathbf{p}_q^T \qquad (4.14)$$

where q = min (m,n), and the $\mathbf{t}_i\mathbf{p}_i^T$ pairs are ordered by the amount of variance captures. $\mathbf{p}_i^T$ is the transpose of $\mathbf{p}_i$. Generally, the model is truncated, leaving some small amount of variance as residual matrix. Therefore, we have following equation.

$$\mathbf{X} = \mathbf{t}_1\mathbf{p}_1^T + \mathbf{t}_2\mathbf{p}_2^T + \ldots + \mathbf{t}_f\mathbf{p}_f^T + \mathbf{E} \qquad (4.15)$$

$$= \mathbf{T}\mathbf{P}^T + \mathbf{E}$$

where

T = scores matrix ($m \times f$) with orthogonal columns, and f is the number of principal components or factors

P = loadings matrix ($n \times f$) with orthonormal columns

E = residuals matrix ($m \times n$) not accounted for by the model

Mathematically, if **X** has been mean-centered, individual loadings, $\mathbf{p}_i$, are the eigenvectors of the covariance matrix, cov(**X**), defined as

$$\text{Cov}(\mathbf{X}) = \mathbf{X}^T\mathbf{X}/(m-1) \qquad (4.16)$$

Thus,

$$\text{Cov}(\mathbf{X})\mathbf{p}_i = \lambda_i \mathbf{p}_i \qquad (4.17)$$

where λ_i is the eigenvalue associated with the eigenvector $\mathbf{p}_i$.

According to Eq. (4.14), matrix **X** can be reduced to a product of two matrices, **T** and **P**. These matrices explain most of the variance in **X**. In equation 4.14, the score vectors, made up of the columns of matrix **T**, contain information on the relationship between the samples. The loading vectors compose of the columns of matrix **P**, which contains information on how variables relate to each other.

The amount of variance captured by $\mathbf{t}_l\mathbf{p}_l$ is proportional to λ_l. For example; the rank-1 outer product of the first corresponding score and loading vector yields a principal component, which explains the contribution of the most significant variance in the data. By properly estimating *f*, the magnitude of the data set size is reduced. The sets of *f* factors, which remain after trimming, are referred to as principal factors or principal components. One easy way to determine *f*, the number of components to retain, is by observing eigenvalues (λ_l) associated with the eigenvector matrix $\mathbf{p}_l$. λ_l shows the magnitude of variance for each factor. The eigenvalues decrease in magnitude for each subsequent factor because smaller and smaller amounts of the total variance will remain undescribed. In all, a set of sample spectra ($m \times n$) can be expressed as the product of **T** and $\mathbf{P}^T$ (the transpose of **P**). **P** can be considered as *f* loading spectra, and each row of **T** as the intensities of each sample represented in the new coordinate system of the *f* loading vectors.

Basically, there are two methods that are often used for the decomposition of **X:** (1) Non-linear Iterative Partial Least Squares (NIPALS) [16,17] and (2) Singular Value Decomposition (SVD) [15] with the latter being a much faster algorithm. These two algorithms differ in the manner in which the eigenvectors of **X** are evaluated. NIPALS calculates one eigenvalue at a time. By SVD, the data matrix **X** ($m \times n$) is decomposed as follows:

$$\mathbf{X} = \mathbf{U}\Sigma\mathbf{V}^{\mathrm{T}} \tag{4.18}$$

Here, the columns of **V** ($n \times n$) (the orthonormal right singular matrix) are equivalent to the PCA loading $\mathbf{p}_i$, the eigenvectors of $\mathbf{X}^{\mathrm{T}}\mathbf{X}$; The columns of **U** ($m \times m$) (the orthonormal left singular matrix) are eigenvectors of $\mathbf{X}\mathbf{X}^{\mathrm{T}}$; and Σ ($m \times n$) is a diagonal matrix. The elements of Σ, $\sigma_1, \sigma_2, \ldots \sigma_r$, are known as the singular values that are placed in a descending order. The singular values are equal to the square roots of the eigenvalues of cov(**X**). Relationship between PCA, SVD, and eigenvectors are given as follows:

$$\mathbf{P} = \mathbf{V} \tag{4.19}$$

$$\mathbf{T} = \mathbf{U}\Sigma \tag{4.20}$$

$$\Sigma_{ii} = \mathrm{sqrt}(\lambda_i) \tag{4.21}$$

The pseudo-inverse of **X**, $\mathbf{X}^{+}$, can be obtained by

$$\mathbf{X}^{+} = \mathbf{V}\Sigma^{+}\mathbf{U}^{\mathrm{T}} \tag{4.22}$$

Σ^+ is the pseudo-inverse of Σ. The reciprocals of the singular values of Σ, $1/\sigma_1$, $1/\sigma_2$, . . . $1/\sigma_r$, are on the diagonal of Σ^+ ($n \times m$). The pseudo-inverse is the same as the inverse, when **X** is invertible.

4.4.2 Partial Component Regression and Partial Least Square Regression

Both Principal Component Regression (PCR) and Partial Least Square Regression (PLS) are factor analysis methods as described in section 4.4.1. One of the common merits of PCR and PLS regressions is to incorporate similar ideas of data reduction, Principal Component Analysis (PCA), in their algorithms.

The regression equation for calibrating the response matrix, **Y** (concentration or other dependent property values being calibrated), against variables matrix, **X** (spectra or other variables), can be written as below:

$$\mathbf{Y} = \mathbf{XB} + \mathbf{E} \tag{4.23}$$

where

X = matrix of size ($m \times n$), the calibration spectra of m samples at n wavelengths ($m < n$)

$\mathbf{Y}$ = matrix of size ($m \times p$), the concentrations of m samples with p pure analytes ($m > p$)

$\mathbf{B}$ = matrix of size ($p \times n$), the spectral coefficients ($p < n$)

$\mathbf{E}$ = matrix of size ($m \times p$), spectra or residuals not fitted by the model

The PCR algorithm is simply PCA followed by a regression step [15]. Based on Equation (4.14), spectral matrix, $\mathbf{X}$, is decomposed into two smaller matrices, $\mathbf{P}_r$ and $\mathbf{T}_r$ (loading matrix and score matrix when the effective rank of $\mathbf{X}$ is r). Actually, $\mathbf{T}_r$ can be obtained according the singular value decomposition given in Eq. (4.18). Then, matrix $\mathbf{Y}$ is regressed against the reduced scores matrix, $\mathbf{T}_r$, by the least-squares regression as follows:

$$\mathbf{Y}_r = \mathbf{T}_r \mathbf{D}_r + \mathbf{E}_r \tag{4.24}$$

$\mathbf{D}_r$ and $\mathbf{E}_r$ are coefficient matrix and error matrix, respectively. In terms of scores, we have

$$\boldsymbol{D}_r = \mathbf{T}_r^{+}\mathbf{Y}_r \tag{4.25}$$

where $\boldsymbol{D}_r$ is a matrix of size ($r \times p$), which indicates the least-squares estimate of $\mathbf{D}_r$ with the sum of squared spectral errors being minimized. $\mathbf{T}_r^{+}$ is the pseudo inverse matrix of $\mathbf{T}_r$, which can be obtained by Equation (4.22)

In terms of original variables, corresponding $\boldsymbol{B}_r$ is given as follows:

$$\boldsymbol{B}_r = \mathbf{X}_r^{+}\mathbf{Y}_r = \mathbf{X}_r^{+}\mathbf{T}_r^{+}\mathbf{Y} \tag{4.26}$$

During prediction, the least-squared solution for the vector of unknown component concentration, $\mathbf{c}_p$, can be estimated from its spectrum, $\mathbf{x}_p$, by using the value of $\boldsymbol{B}_r$ estimated in Eq. (4.26) as follows:

$$\mathbf{c}_p = \mathbf{x}_p \boldsymbol{B}_r \tag{4.27}$$

In PCR, the score vector corresponding to relative small eigenvalues are left out in order to avoid sensitivity problem caused by collinearity. Thus, this regression gives no matrix inversion problems. However, PCR only uses the **X** matrix to determine the linear combination of variables. The concentration **Y** matrix is used to estimate the regression coefficients rather than **T** to determine which part of matrix **X** to throw away. A potential disadvantage of PCR is that variation in **X** that is not correlated with the concentration of interest may be used to construct **P**. Sometimes, the variance, which is related to the concentrations, is a very small portion of the overall variation and may be thrown away during the step of determining how many factors to keep. If this is the case, PCR may fail to find the optimum linear combinations of variables for modeling the concentrations.

The approach taken by PLS is very similar to that of PCR, except that factors are chosen to capture the correlation between **Y** and **X**. This is accomplished by using the columns of the **Y** matrix to estimate the factors for **X**. At the same time, the columns of **X** are used to estimate the factors for **Y**.

The **X** and the **Y** matrices are decomposed in the following manner [15]:

$$\mathbf{X} = \mathbf{T}\mathbf{P}^{\mathbf{T}} + \mathbf{E} \tag{4.28}$$

$$\mathbf{Y} = \mathbf{U}\mathbf{Q}^{\mathbf{T}} + \mathbf{F} \tag{4.29}$$

where, the elements of **T** and **U** are the scores of **X** and **Y**, respectively, and the elements of **P** and **Q** are called the loadings. **E** and **F** are the errors. The decomposition as defined by equations 4.28 and 4.29 based on describing maximum correlation between **X** and the **Y**.

PLS uses concentration information to obtain the decomposition of spectra matrix **X**. Concentration-dependent loading vectors have generated **P** and the computed scores, **T**, are then related to the concentration or concentration residuals after each loading factor is calculated. Therefore, in principle, greater predictive

ability is forced into the PLS loading vectors. The application of PCR and PLS in spectral analysis has been widely reported [15-17].

Additionally, regarding PLS there are two approaches that can be used to develop a calibration model if there is more than one analyte of interest. For the approach termed PLS1, separate models are developed for each analyte. For PLS2, a single model is built for all analytes simultaneously. This second approach complicates the selection of the rank or the number of components because it, sometimes, is difficult to select a rank that is optimal for all analytes.

4.4.3 Diagnostics of PCR and PLS Models

For a successful prediction, a calibration model should contain the regression coefficients and the number of the factors. Basically, for a typical calibration, there are two steps to build up a calibration model. First, a calibration model or the regression coefficients are developed using a set of samples with known properties (called calibration set). Then, the calibration model predicts a different set of samples (called prediction set), and the optimal number of factors is selected according to the prediction error. The prediction error is expressed as Predicted Residual Sum of Squares (PRESS) [15].

$$\text{PRESS}_j = \sum_{i=1}^{N} (\hat{y}_{i,j} - y_i)^2 \qquad (4.30)$$

where

j = number of factors included in the calibration model

y_i = actual value of the i-th sample in the prediction set

$\hat{y}_{i,j}$ = predicted values of the i-th sample (in the prediction set) for the calibration model built with j factors

N = number of samples used in the prediction set

Using models containing different number of factors, a series of PRESS values from predictions are obtained. Based on the plot of PRESS vs. the number of factors, the optimal number of factors is the one, which leads to minimum PRESS. In principle, using fewer principal components in the calibration model may exclude important information from the model, and this would lead to an insufficient calibration model; using too many factors would incorporate redundant information and random noise, and this makes the model highly unstable and produce higher prediction errors in the prediction.

If there are not enough samples available to obtain a prediction sample set, a compromise approach, cross-validation procedure, can be used to determine the optimal number of factors for a PCR or PLS calibration model [15,16]. In a cross-validation modeling procedure, a group of samples (containing one or more than one

samples) from the calibration set is temporarily left out from the calibration sample set. Then the remaining samples are used to create a model to predict the properties of the samples removed and the residual is recorded. The removed samples are then included in the calibration model, and a different subset is excluded from the calibration and used as prediction sample set. This procedure is performed till all the samples have been left out once. Similarly, the optimal number of factors can be identified from the obtained plot of combined PRESS vs. the number of factors.

PRESS only shows the magnitude of prediction error for the whole prediction sample and will increase with rising sample number in the prediction set. In the estimation of the prediction error, it is essential to show how many samples are used in the prediction set, and the PRESS values should be converted into units of the measurement. The model error in the predictions of the samples in the prediction set is termed as the Standard Error of Prediction (SEP) [15].

$$SEP = (PRESS/N)^{1/2} \tag{4.31}$$

where N is the number of samples used in the calibration set. SEP is also a function of the number of factors and can be used to estimate the optimal number of factors for the model.

The SEP value quantitatively estimate the accuracy of the calibration models. They depend on the analyte level, the inherent accuracy and precision of referenced samples, and the stability and reproducibility of the instrumental measurement. It is considered reasonable that the predictions for an unknown sample using the calibration model lie within ± SEP limits of the true value and that the properties of the unknown sample cannot be accurately predicted if its concentration is lower than SEP value. Thus, the SEP can be utilized for setting control limits or detection limits in a real-time monitoring processes.

Chapter 5

Review of Spectrometric Techniques for Characterization of Crude Oil and Petroleum Products

In this chapter, a review of the spectrometric techniques used to characterize petroleum and its product has been discussed.

5.1 Crude Oil & Shale Oil

Kvalheim et al. [18] have applied PCA to ^{13}C NMR spectra of the naptha fraction of crude oil from wells located on the Norwegian shelf. Principal Component Analysis (PCA) correlates oil samples from the same geographical area. The correlation follows from the properties related to the composition of the oils, e.g., long chained versus short chained alkanes, branching, cyclization, and aromatization. Several of the major constituents present in the oils were identified. Ali et al. [19] have used ^{1}H and ^{13}C NMR spectra of asphaltenes separated from heavy crude oil using n-pentane. Average molecular parameters and hypothetical structural models for these asphaltenes were proposed using NMR measurements, calculated molecular weight of unit sheets and elemental analysis. Zhendi [20] and associates have developed a rapid and reliable method for fractionation of oil into

aliphatic and aromatic hydrocarbons using 3-g silica gel micro glass chromotographic column. Upto 50 mg of oil can be quantitatively fractionated. The resulting fractions were analyzed by capillary gas chromotography coupled with flame ionization detection and gas & mass spectrometry. Many detailed structural features of substituted napthenic, naptheno-aromatic, and mono- and di-aromatic carboxylic acids from a California crude oil have been elucidated after isolation of fractions of derived hydrocarbons by repeated chromatography on alumina and the application of a variety of methods of high resolution molecular spectrometry [21]. The analytical methods involved were a combination of computer-averaged nuclear magnetic resonance, high-resolution mass spectrometry, ultraviolet, fluoroscence and infrared spectrometry, and gas chromatography combined with low-resolution mass spectrometry. This comprehensive approach has resulted in compound class identification of many types of carboxylic acids which, have not been reported previously in petroleum. Downare et al. [22] have studied the visible and near infrared fluoroscence of crude oils. In their work they have measured the fluoroscence emission spectra for ten diverse crude oils at various concentrations over a broad range of excitation and emission wavelengths in the visible and the near infrared. Their study indicates that all crude oils possess the same chromophores and fluorophores, but in very different concentrations. Differential Scanning Calorimetry (DSC) has been used to characterize crude petroleum [23]. A thermal fingerprint can be obtained in a short time with a single experiment. Several parameters such as the

glass transition temperature of the hydrocarbon matrix, temperature of crystallization and paraffins content can be measured with good reproducibility. Felix and associates [24] have focussed on the development of different type of HPLC stationary phases for performing hydrocarbon group type analysis. Orbey and Sandler [25] presented models for calculating the viscosity of hydrocarbon and their mixtures including crude oils over a wide range of temperature and pressure. The model is predictive and requires the normal boiling point of the constituents as inputs. Miadoyne et al. [26] presented a correlation for the effect of temperature on the kinematic viscosity of crude oil fractions which requires one measurement on each fraction at 100F. Coal liquids have been distilled and chemical structural correlations have been determined as a function of boiling ranges by Yokayama et al. [27]. Pruski et al. [29] have studied the chemical functionalities of hydrogen and carbon in a series of coke obtained from heavy crude oils in Mobil continuous flow laboratory coker pilot plant with high resolution solid state NMR. The high resolution spectra in combination with previously reported wideline ^{1}H NMR data and the results of the elemental analysis were used to derive several structural parameters including aromatic and aliphatic hydrogen to carbon ratios and the average formula per 100 carbon atoms. It was concluded that most cokes consist of molecules having approximately 10 aromatic rings bearing only few substitutions. McAskill [29] has done photoacoustic study on a number of Australian coals of widely varying rank and various oil shales in near infrared (NIR). He concluded that

the NIR spectra of many coals and oil shales are featureless because of strong background due to electronic adsorbtion.

5.2 Fuel Fractions (gasoline, diesel, and kerosene)

An understanding of the hydrocarbon type compositions of fuel fractions (gasoline, diesel, and kerosene) is essential for research and development of production process, product quality determination and, also in deciding their industrial utilities. The importance of gasoline composition determination is further emphasized by the higher participation of gasoline from secondary processes in motor gasoline formulation, by higher quality standards, as well as by increasing the requirements in environment consideration. It has been claimed that the aromatic species in diesel fuel play a significant role in the formation of particulates and there are proposals in some areas to limit the aromatic content of automotive diesel fuel [30]. The kerosene fraction is primary source for production of Aromatic Type Fraction (ATF), naphthalenes and their precursors for dyes and intermediate industries and feed stocks for alkyl-benzenes for biodegradable detergents [7]. The producing process for dearomatizing kerosene fractions by solvent extraction to produce ATF requires a fast and accurate method for estimation of total aromatics in the feed and its various fractions.

Although the fluorescent indicator adsorption (FIA) method is being used as the standard method in the petroleum industry for estimation of paraffinic, olefinic and aromatic contents in fuel fractions,[31] its drawback has been well recognized. It requires long analysis time and much operator attention, and can not perform individual component analysis and carbon number distribution. A number of methods of fuel fraction composition determination have been developed. They provide determination of individual components of fuel fraction, or the type of hydrocarbons, or the functional groups. These methods are based on gas chromatography, high performance liquid chromatography, Infrared spectrometry, NMR Spectroscopy, Raman spectroscopy, and second derivative ultraviolet spectroscopy. Details of these methods will be presented, respectively.

Kosal, N. [8] and others applied gas chromatographic techniques including capillary (CC-gc) and valve switching multiple packed column (MC-gc) as well as standard ASTM FIA method in identification of hydrocarbon types for paraffins, olefins, naphthenes and aromatics (PONA) in petroleum fractions. The degree of information obtained increases from FIA to MC-gc to CC-gc. FIA gives total hydrocarbon types, MC-gc reports the carbon numbers, and CC-gc gives information on each individual component. The Institute of Petroleum has developed two methods for determining the aromatic content of diesel fuels: total aromatic content by High performance Liquid Chromatography with refractive index detection

IP391/90 and aromatic carbon content by High resolution ^{13}C Nuclear Magnetic Resonance Spectroscopy [30]. Derivative ultraviolet spectroscopy has been applied to aromatic hydrocarbons. The additional degree of freedom offered by the derivative technique has been employed for the qualitative estimation of total aromatics in food-grade hexane and lighter petroleum fractions.

Ramaswamy, V. and others [7] derived a general equation for the quick and accurate estimation of total aromatics in straight run kerosene fractions by using IR absorbance from aromatic concentrates of kerosene in different crude oils. The characteristic wavenumbers for the IR absorbance were 1610, 810, 785, 745 and, 705 cm^{-1}. The accuracy of the method was ± 5%, and the deviation from the standard FIA method was within 5.5%. A new analytical method based on midband Fourier transform infrared spectroscopy has been developed that allows for rapid and reliable measurement of several pertinent fuel properties simultaneously [6,10]. The selected properties were aromatic hydrocarbon content, carbon-to-hydrogen ratio, heat of combustion, cetane index, viscosity, density, etc.. Midband FTIR spectroscopy, when combine with multivariate calibration analysis, is a versatile, efficient, and accurate technique for estimating several important fuel properties. This new methodology could increase the corresponding output of the petroleum laboratories by a factor of over 200 to 1, while maintaining data integrity and minimizing sample requirements, environmental hazards, and cost.

As early as 1950, Raman spectroscopy was proposed as a method to determine aromatics and olefins in hydrocarbon mixtures. However, extensive use of Raman spectroscopy is limited by the presence of fluorescence in hydrocarbon fuels when excited by visible lasers. The development of FT Raman spectroscopy, using a near-infrared laser source, overcomes many fluorescence problems. Recently, Raman spectroscopy has been used in the qualitative analysis of turbine fuel for the determination of general hydrocarbon makeup, aromatic components, and additives presence [32]. In addition, Seasholtz and others have shown that near-IR FT-Raman spectroscopy is suitable for qualitative analysis of the percentage of liquid fuel mixtures containing unleaded gasoline, superunleaded gasoline, and diesel using multivariable techniques [33]. Willams and co-workers [34] have demonstrated that near-IR FT-Raman spectroscopy in combination with multivariate calibration can be used for determine gas oil cetane number and cetane index. Cooper and others [35] have demonstrated that Near-IR FT-Raman spectroscopy in combination with partial least-squares regression analysis can be used to construct highly correlated models relating a petroleum fuel's Raman spectrum to its motor octane number, its research octane number, its pump octane number, and its Reid vapor pressure. Raman spectroscopy has demonstrated ability to quantitate octane numbers and vapor pressure across a diverse range of fuel compositions with a single multivariate model for each property being quantified. This capability has not been

demonstrated with near-IR spectroscopy. Raman spectroscopy has demonstrated advantage of being able to quantitatively determine chemical species in hydrocarbon blends where near-IR analysis failed [36].

In the functional group analysis of the complex hydrocarbon compounds in gasoline, NMR spectroscopy has a distinctive position. Srica, V. and co-workers [37] have demonstrated that NMR can be successfully applied to content determination of aromatic, olefinic, and paraffinic hydrocarbons of high-olefin coking gasoline without separation. Deviation of the NMR spectroscopy results from the standard method is within the repeatability limits for the standard method. The method is significantly faster. It provides not only data on composition by hydrocarbon types but also data on structural characteristics from the same analysis. Caswell and others [9] presented a method of directly coupling liquid chromatography ^{1}H nuclear magnetic resonance for rapid prediction of various physical properties for middle distillate fuels. The physical properties that can be obtained in this manner are cetane number, cetane index, density, specific gravity, pour point, volume percent aromatics, residual carbon content, and the initial, 10%, 50%, 90%, and end boiling point. The method also provides chemical insight concerning the influence of chemical structural changes on the physical properties of the fuel as well as requiring less analysis item and sample volume than the corresponding standard ASTM methods. This technique is especially suitable to the

situation that a large number of physical properties of a limit amount of fuel sample are required in a very short period time.

5.3 Lube Oil

Singh et al. [38] have studied the average molecular structures of eighteen lubricating oil base stocks, prepared from Darius crude oil in spindle, intermediate and heavy viscosity ranges using elemental analysis, molecular weight, and NMR spectroscopic data. The structures obtained have been found to be sensitive to the degree of refining and type of finishing (clay or hydro) even within the same series. They have discussed the importance of the average molecular structure of the lubricating oils in relation to their physico-chemical properties. Brant and Kiviat [39] have developed a method for the rapid determination of total aromatic molecules in the light lube oil distillates and two types of finished oils by infrared spectroscopy utilizing a microprocessor controlled spectrometer. This method is also good for solvent extracted process intermediates. Wiseman and Ah-Sue [40] have used Fourier Transform Infrared (FTIR) spectroscopy to monitor the chemical composition of lubrication oils. It provides a reliable method whereby degradation products and non-metallic contaminants can be closely analyzed. They also describe a method by which the infrared spectra can be used to determine its condition as well as contamination by external agents. They have developed an expert system so as to

automate the interpretation of a large number of spectra. Stuart et al. [41] have examined used lubricating oils by a number of spectroscopic techniques to assess whether it might be possible to improve turn-around time for laboratory analysis or to develop a simple oil quality sensor which could be used in a service workshop. They showed that the development of an oil quality sensor based on a discrete wavenumber measurements in the mid-infrared region would not be warranted, but heptane-insolubles can be estimated from a single measurement in the near-infrared region, and this could form the basis of a simple sensor. Kushnarev et al. [42] have used NMR spectroscopy to monitor molecular composition and structure in the feedstock and products from the traditional stages employed in producing distillate base oils (selective purification with phenol, deparaffinization in an MEK-toluene solution, and hydrofining) with three fractions of commercial low-sulfur Western Siberian Crude as a model. The potential base oil content and quality in the test fractions were determined by adsorptive separation. A separation scheme followed by GC/MS was developed to determine the concentrations of mono- to tetra-cyclic aromatic hydrocarbons in lubricating oils [43]. An improved proton NMR method was developed for the determination of aromatic carbon content in the base oils and middle distillates [44], and NMR was also used in another study to explain structural changes during the hydrogenation of lubricant distillates [45].

5.4 Heavy Fractions

Yen et al. [46] have studied the structure of petroleum asphaltenes using infrared. They have shown that heat treatment of petroleum results in the appearance of chain like condensed napthenic structure in asphaltenes. Condensed napthenic groups were shown to be present and to vary with the source of crude oil and it's treatment prior to the separation of the asphaltic fraction. The proportions of the total number of carbons existing in the napthenic, paraffinic and, specifically, as terminal methyl groups have been estimated. Khorasheh et al. [47] have developed the Structural Group Analysis (SGA) for the characterization of Alberta gas oils. The gas oils were separated into class fractions enriched in selected structural groups. Data from elemental analysis, ^{1}H NMR, ^{13}C NMR and infrared spectroscopy were used in an optimization procedure to obtain the group concentrations. Kotlyar and associates [48] separated the solids associated with bitumen derived from a variety of oil-sand grades into fractions having different humic matter content by means of density fractionation. For all humic acids analyzed, the elemental composition and distribution of the carbon types in each region of ^{13}C NMR spectra were similar. It was shown that the aromatic carbon was the predominant type of carbon for all samples. Hasan et al. [49] carried out the separation and characterization of asphaltenes from the four marketable Saudi Arabian crudes by various analytical techniques. Asphaltenes were precipitated by adding excess n-pentane to heavy end

of each crude. They have used elemental analysis, spot tests, molecular weights, phenol interaction values and, infrared spectroscopy for characterization. Infrared spectra showed the presence of several types of functional groups. A study was made using NMR spectroscopy on visbreaker (VB) and straight-run bitumens to find the structural differences [50]. The results showed that the aromatic carbon and hydrogen contents are appreciably higher in VB bitumens, thus aiding characterization. Kaihara et al. [51] have described a novel measurement techniques for Fourier transform infrared spectrometry, namely scattering filter method and scattering dilution method combined with ellipsoidal mirrors for detailed analyses of the structure of highly scattering samples, for example, petroleum pitch and coal slurry. The technique provided excellent spectra of low background, high signal to noise ratio and high signal to background ratio, sometimes detecting new bands which had not been reported previously by the use of the conventional KBr pellet method. Ram et al. [52] have identified various molecular species present in Athabasca oil sand using X-ray powder diffraction, and infrared and Raman spectroscopy (200 - 4000 cm^{-1}). They found that acyclic paraffin, straight chain alkanes, and sterane hydrocarbons were prominent. The infrared spectra and hydrogen bonding effects in asphaltenes and resin fractions of Athabasca bitumen have been investigated [53]. Philip and associates [54] have used NMR and FT-IR to evaluate the efficiency of Corbett separation and also, to study the predominant structural features of asphalt and it's Corbett fractions. The determination of the

relative percentage of paraffinic, napthenic and, aromatic carbon in oil fractions by ^{13}C NMR has been shown to compare well with the results from ASTM D2140 procedures [55]. In the ASTM method the PNA analysis is determined by the refractive index, the density and the molecular weight of the material. In ^{13}C NMR spectroscopy, the carbon types are directly observed and under appropriate conditions can be readily quantified [55-57]. Aromatic carbon resonance is observed in the 110-170 ppm region of the 25-60 ppm region of the spectrum. The paraffinic carbon signals are seen as a band of overlapping resonance in the 0-25 ppm region and as sharp resonance in the 25-60 ppm region. Ali et al. [58] have presented the results of separation and characterization of asphaltenes, resins and, oils from four Saudi Arabian crude oil residues by NMR and infrared methods. Yokoyama et al. [59] have done the structural characterization of heavy crude oil derived from coal hydrogenation by proton and ^{13}C NMR. Haley [60] has studied the molecular and unit sheet weights of asphalt fractions separated by gel permeation chromatography. Nuclear magnetic resonance unit sheet weights were determined for fractions of both the asphalt and asphaltene. The study suggests that the asphaltene molecules consist of a number of unit sheets attached together rather than one large pericondensed (condensed at 1,8 or 4,5 sites of the ring structure) aromatic ring system. Hayes et al. [61] have used dielectric constant detector for high performance liquid chromatography for the rapid and accurate hydrocarbon group analysis. The DC detector ensures genuine uniformity of response for each hydrocarbon group

independent of the carbon number distribution of the sample thus enhancing the quantitative accuracy of HPLC technique. Ramaswamy and associates [62] have studied the compositional and structural data of North Gujarat mix vacuum gas oil by employing separation procedures and instrumental techniques, viz. IR, NMR and MS. Among the different types of hetroatomic functionalities estimated by infrared spectroscopy, phenols are found to be predominant and are followed by carboxylic acids. Various average structural parameters of saturate and aromatic subfractions have been derived using proton and ^{13}C NMR spectroscopy [62]. The comparison of structural parameters calculated by ^{1}H NMR, IR, Brown Ladner and n-d-M (refractive index-density-molecular weight) methods were carried out for six heavy oils [63]. It was proposed that the ^{1}H NMR/IR method give more precise average molecular parameters than the Brown Ladner method. N-d-M method gives correct molecular structural parameters for some heavy oils with lower molecular weight, but the information of the molecular structure obtained from it is limited. Ali et al. [64] studied the residue from Arabian Heavy Crude Oil by separating it into four fractions, asphaltenes, resins, aromatics and saturates. And characterizing each fraction by elemental analysis, infrared spectroscopy, NMR spectroscopy and mass spectroscopy. The structural characterization led to the conclusion that asphaltene fraction is maximum hydrogen deficient followed by resins, aromatics and saturates, thus suggesting larger degree of ring condensation in the structure of asphaltenes than the resins and aromatics. Netzel et al. [65] have come up with correlations for

viscosity of US tar sand bitumen with NMR spectroscopic parameters. The method is semiempirical, but is based upon some fundamental theoretical concepts of molecular mobility and intermolecular interaction. Bukka et al. [66] studied the influence of carboxylic acid content on bitumen viscosity for six diverse tar sand deposits by FT-IR and specular reflectance FT-IR. Although it was shown that bitumen with higher viscosity generally contained larger quantities of carboxylic acid, a simple quantitative relationship between two would be difficult to obtain with the exclusion of other parameters. The viscous nature of bitumen is principally attributed to the internally suspended asphaltenes. However, the fractional compositions also indicated that the viscosity of given bitumen cannot always be attributed to asphaltene content alone. Zerila and associates [67] have used the method of partial least squares modeling in latent variables to relate the ultraviolet spectral parameters to the saturates content of heavy petroleum products without the need for prior deasphalting or chromatography. They have presented statistical evaluation and results for reference aromatic mixtures, artificial samples and, actual petroleum fractions.

5.5 Conclusions

Infrared absorption spectroscopy (IR) may offer valuable information about the hydrocarbon skeleton and about the functional groups in petroleum. Qualitative

information on specific structural elements can be obtained even though the spectra are too complex for individual compound analysis. For example:

a. IR is extensively used in the elucidation of the structural entities present in asphaltenes resins, and oils in crude oil residues [58].

b. IR is also used to identify various functional groups including hydroxyl (3450 cm^{-1}) and carbonyl (1695-1725 cm^{-1}). One of the most beneficial uses of IR is in the study of hydrogen bonding in petroleum [68].

c. FT-IR has been used to monitor the chemical composition of lube oils. It provides a reliable method whereby degradation products and non-metallic contaminants can be closely analyzed [40].

d. FT-IR, when combined with multivariate calibration analysis and regression equation, may be used for measurement of several pertinent fuel properties, such as aromatic, olefinic, and saturated hydrocarbon content, carbon-to-hydrogen ratio, heat of combustion, cetane index, viscosity, density, etc. [6,7].

Nuclear Magnetic Resonance (NMR) has proved to be of great value in Petroleum research because it can identify the chemical nature of hydrogens and carbons even in complex organic mixtures of petroleum and its refinery products [54]. Since the major constituents in crude oil are made up of rather few molecular fragments, ^{13}C

NMR spectroscopy produces spectra with well-resolved parts even from fractions containing a large number of constituents. ^{13}C NMR spectroscopy has become a useful tool in the analysis of crude oils and petroleum products [69]. Proton NMR allows rapid and nondestructive determination of the total hydrogen content and distribution of hydrogen among the chemical functional groups present in the sample. The technique is also useful as a means of estimating molecular weight and for studying processing effects [68]. For example:

a. Principle component analysis (PCA) has been applied to 13C NMR spectra of the naphtha fraction of crude oil. Several of the major constituents (pentane, hexane, heptane, benzene, etc.) present in the oils have been identified [18].

b. A set of 15 petroleum cokes produced by delayed coking in a Mobile laboratory coker has been studied using solid state ^{1}H NMR. From solid echo and free induction measurements, the concentrations of hydrogen were measured [70].

c. With the help of instrument analysis such as ^{1}H NMR, IR, and ^{13}C NMR, many methods have been proposed to calculate structure of heavy oils [63].

d. NMR spectroscopy combined with elemental analysis and molecular weight has been used to determined the average molecular structure of eighteen lube oil base stocks [38].

e. A method has been developed whereby the viscosity of a tar sand bitumen can be calculated from NMR parameters [65].

f. ^{1}H NMR has been successfully applied in content determination of aromatic, olefinic, and paraffinic hydrocarbons of high-olefin coking gasoline without separation. The method is significantly faster, it provides not only data on composition by hydrocarbon types, but also data on structural characteristics from the same analysis [37].

g. A method of directly coupling liquid chromatography/ ^{1}H NMR has been developed for rapid prediction of various physical properties (such as cetane number, pour point, volume percent aromatics, residual carbon content, etc.) for middle distillate fuels. The method also provides chemical insight concerning the influence of chemical structural changes on the physical properties of the fuel [9].

h. A method is reported that for the identification of the aromatic components of four intermediate boiling (175.5-254 °C) crude oil fractions analyzed by short- and long-range heteronuclear shift correlation 2D NMR spectroscopy. The method provides reliable data which are needed for the thermodynamic simulation of crude oils in the boiling temperature range where the usual 1D methods alone are not entirely satisfactory [71].

Chapter 6

Experimentation and Analysis

6.1 Background

The work presented in the thesis is sponsored by Top Source Instruments Inc.. The project was focused on developing feasible technologies that can be incorporated into an instrument for the rapid characterization of heavy oil fractions. This instrument would be used either on-line or off-line for process monitoring and quality control of the refinery products. The technology would replace the time and labor intensive characterization techniques presently used in the refinery labs. The incorporation of this instrument in refineries would reduce the labor and maintenance involved in the quality control labs in the industry. The time scale of characterization by the instrument will be of the order of 2 minutes and hence, the results can be used more effectively for process feedback. This is in stark contrast to the time taking characterization techniques prevalent in the industry.

Top Source Instrument Inc. is a subsidiary of Top Source Technologies focusing on oil analysis. The company developed an On-Site Analyzer (OSA) to monitor the condition of used lubricating oils in engines and transmissions. This

instrument involves the integration of an optical arc emission spectrograph and a transmission Fourier Transform Mid-Infrared (FTIR) spectrometer that provide data that is used to assess mechanical wear (metal analysis) and oil analysis (chemical analysis). In the original version of this analyzer, the used oil was automatically transferred between the spectral instruments by a pumping system.

For refinery applications the instrument was modified to accommodate heavy oil fractions. This required changes in the measurement methodology and also required changes to the sample handling system. The latter changes, which required heated transfer lines, were necessary because the heavy oil fractions are semi-solid at room temperature. In terms of the methodology, the metal analysis was modified to include elements important to lube oil production, such as Chromium, Iron, Nickel, Vanadium, Molybdenum, and Sodium. Likewise, the infrared analysis (FTIR) was changed to provide a measurement of parameters important in lube oil production, and these included viscosity at 100 ^{0}F and 210 ^{0}F, viscosity index, color, flash point, and specific gravity.

Typically, infrared does not provide information that is directly related to these parameters. However, it does provide information regarding the chemical composition, and in turn this information can be linked to the physical properties by the use of modeling techniques, known as chemometrics. This technique has been

discussed in detail in section 4.4. A modified OSA for refinery application, known as OSA-R, was produced based on these measurement principles. A schematic of the original OSA-R can be seen in Figure 6.1. The FT-IR spectrometer in the OSA-R is a Impact 400 from Nicolet and its description is listed in Table 6.1. Transmission infrared sampling technique is used with a optical cell of path-length 400μ.

The key parameters of the used lube oil that were being modeled by the OSA-R were as follows:

- Metal content in ppm for Chromium, Iron, Nickel, Vanadium, Molybdenum and Sodium
- Viscosity Parameters : Viscosity at 100 ^{0}F and 210 ^{0}F, and Viscosity Index
- Color
- Flash point
- Specific gravity

This modified OSA-R was considered appropriate for the off-line monitoring of refinery process streams, in particular for lube oil fractions. The predictions of important oil properties by the OSA-R were not satisfactory. After about 18 months of experimentation at a refinery, the OSA-R did not meet expectations. A research program was initiated at the University of Tennessee, Knoxville (UTK) to evaluate the OSA-R technology, and to recommend alternative approaches.

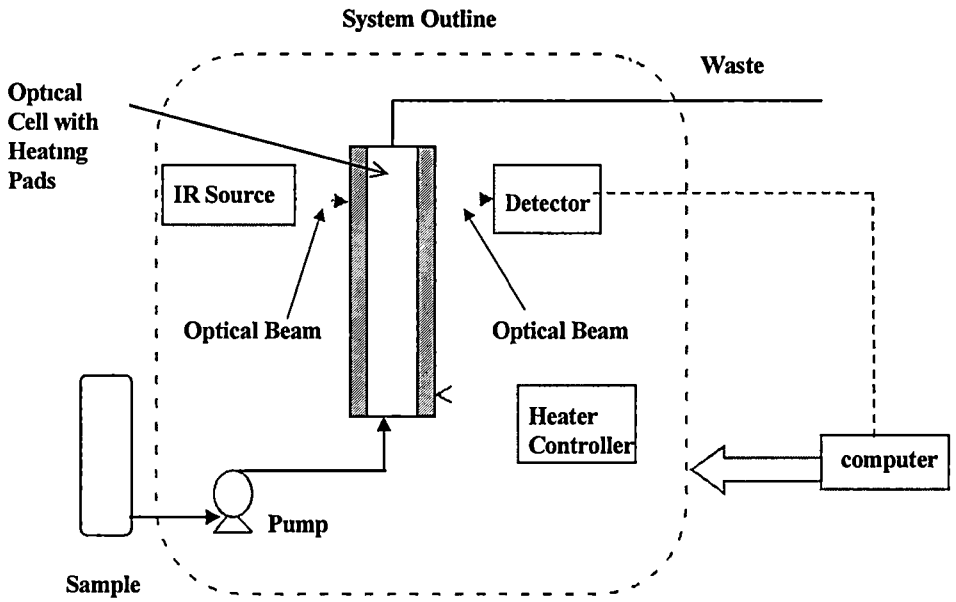


Figure 6.1 Schematic of the On-Site Analyzer-Refinery (OSA-R) version

Table 6.1 Description of the Impact 400 FT-IR spectrometer from Nicolet.

Spectrometer	Impact 400
IR source	Ever-Glow (glowing filament)
Detector	DTGS
Beamsplitter	KBr
Laser frequency	15798 cm^{-1}
Interferogram peak position	1024

6.2 Sample Description

The Top Source Instruments provided the samples for the experiments. These were the lube oil fractions from a refinery. These are the fractions obtained from the vacuum distillation column and the bottoms of the atmospheric distillation column. These fractions in general have a boiling point above 400 ^{0}C. The samples were dark and mostly solid or semi-solid at room temperature. Table 6.2 provides typical physical properties for a representative set from the samples. The samples belonged to different stocks in the refinery. The stock depends upon the type of the distillation column (atmospheric or vacuum) and the level in the column from where they are extracted. The stock was named as 7V2 or 9A5 etc.. Stock 7V2 signifies that the stock originates from a column number 7 which is a Vacuum distillation column and the fraction is cut at level 2. Similarly, stock 9A5 signifies that the stock originates from column number 9 which is a Atmospheric distillation column and the fraction is cut at level 5 and so on. This nomenclature was given at the refinery. For convenience, these samples were renamed in our lab. Each sample was assigned an alphabet depending on which stock it was from. The alphabet was followed by a number that differentiated the samples of the same stock from each other. Primary measurements of the physical parameters of some of the samples were provided to us.

Table 6.2. Physical properties of few of the representative samples. The values were provided by the quality control lab at the refinery.

S.No.	UT ID	Stock ID	V_{100} (ssu)	V_{210} (ssu)	VI	COLOR
1	a1	7V2	159.4	42.7	69	9.3
2	d1	7A4	115.7	40	79	11.1
3	d4	7A4	144	41.8	76	10.5
4	g3	8V1	185.6	44.5	79	11.9
5	g5	8V1	202.7	45.5	80	11.1
6	i6	8V2		72.5		8.7
7	i9	8V2		63.7		9.6
8	i11	8V2		66.3		8.1
9	k2	8V3		99.5		2.6
10	k6	8V3		93.5		3.5
11	k8	8V3		89.2		4.5
12	n1	9V1	221.2	45.5	62	10
13	n6	9V1	237.8	46.1	56	10
14	p1	9V2		76.7		7.2
15	p5	9V2		76.4		8.1
16	s1	9A5	119.7	39.8	56	11.9
17	s6	9A5	146.3	41.47	60	10.5

UT ID is the nomenclature given to the samples at University of Tennessee. Samples belonging to different stocks were assigned different alphabets.
Stock ID This is based on which column (atmospheric {A} or vacuum {V}) and the pipestill the sample originated.
$\mathbf{V_{100}}$ is the viscosity of the sample at 100 ^{0}F.
$\mathbf{V_{210}}$ is the viscosity of the sample at 210 ^{0}F.
VI is the viscosity index of the samples

6.3 Test Run on OSA-R Analyzer

6.3.1 Performance of the Original OSA-R Analyzer

Initially the samples were tested on the OSA-R analyzer to review its performance and its weakness. The predictions from OSA-R for the properties of these samples were in general inaccurate. Viscosity and viscosity index were predicted higher than their true values. Similarly, the color predictions were not close to the expected values. The difficulties in color and flash point predictions were anticipated because they are not directly related to the information in the IR spectra. Also, the concentration of the species (aromatics and asphaltenes) which imparts the color to the samples was too low for the reliable FTIR prediction. Visible spectroscopy would be a better method for color characterization since it is directly related to the color of the sample.

6.3.2 Remodeling of the Chemometrics of OSA-R Analyzer

In the original OSA-R, the modeling of the physical properties (chemometrics) was very complex. Multiple models were used to predict a single property of the samples. For example, VI predictions for samples originating from

different stocks were predicted using different calibration models. This led to the over-fitting of the data, thus making the models unreliable and less robust.

As a first step towards improving the original OSA-R, the chemometric models in the OSA-R were modified while maintaining the original FTIR instrument configuration. Multivariate predictive models using Partial Least Squares (PLS) were built. Initially, two physical properties: (1) viscosity at 100 ^{0}F (V_{100}), and (2) viscosity at 210 ^{0}F (V_{210}) were modeled. These models were based on the FTIR spectral data from the original OSA-R. The models had four Principal Components (PC). Prediction of a particular property, such as V_{100} for all the samples, was achieved using a single model rather than using multiple models as was the case with the original system. The results from these new models can be seen in Figure 6.2 & 6.3 and Tables 6.3 & 6.4. We observe that the prediction for V_{210} is generally within 10% of the actual values. The Standard Error of Prediction (SEP) is 3.29. The V_{210} of the samples varies from 40 to 100 ssu. For this range of prediction, the SEP value of 3.29 at this stage is considered acceptable. This is an improvement over the results that were obtained from the original OSA-R models. However, the prediction of V_{100} was still not satisfactory. One caveat is that the models were generated from a limited sample set, and at this point the general applicability is unknown.

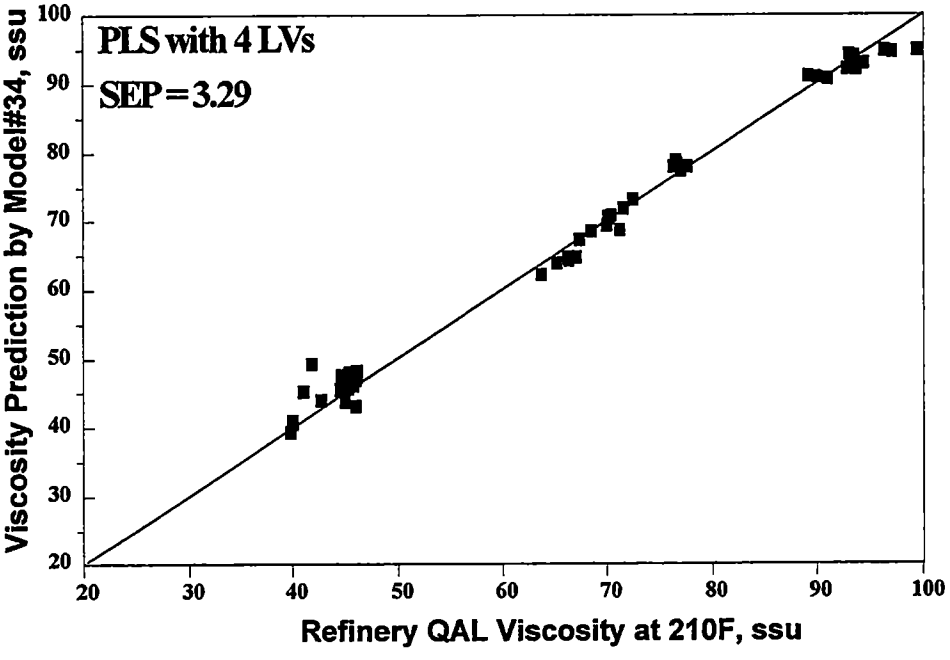


Figure 6.2 Partial Least Squares model for viscosity at 210 ^{0}F. Model is based on the infrared spectra obtained from OSA-R with the optical path-length of 400μ. 4 principal components were used and the SEP value was 3.29.

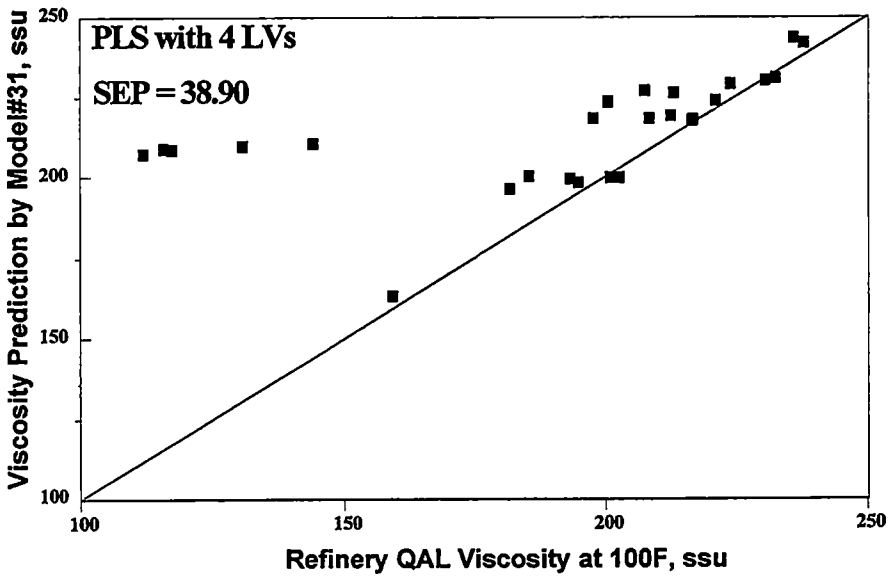


Figure 6.3 Partial Least Squares model for viscosity at 100 ^{0}F. Model is based on the infrared spectra obtained from OSA-R with the optical path-length of 400μ. 4 principal components were used and the SEP value was 38.90.

Table 6.3 Prediction of viscosity at 210 ^{0}F. The model is based on IR spectral data collected from 400μ cell in the original OSA-R analyzer. SEP value is 3.29.

S.No.	UT ID	Stock	Refinery measured viscosity at 210 ^{0}F (ssu)	Model predictions (ssu)	Percent deviation
1	a1	7V2	42.7	42.72	-0.05
2	a2	7V2	46	46.51	-1.12
3	a3	7V2	45.6	45.42	0.39
4	a4	7V2	45.8	44.45	2.95
5	a5	7V2	45	42.22	6.18
6	a6	7V2	46	42.00	8.70
7	a7	7V2	45.4	47.17	-3.90
8	a8	7V2	45.6	45.72	-0.27
9	d1	7A4	40	38.94	2.66
10	d2	7A4	40	38.50	3.75
11	d3	7A4	39.7	37.19	6.31
12	d4	7A4	41.8	47.72	-14.16
13	d5	7A4	41	43.68	-6.53
14	g1	8V1	44.7	45.40	-1.57
15	g3	8V1	44.5	43.07	3.21
16	g5	8V1	45.5	44.23	2.78
17	g6	8V1	45.4	43.46	4.26
18	g7	8V1	44.9	44.26	1.42
19	g8	8V1	44.5	43.11	3.13
20	g10	8V1	45.8	44.08	3.75
21	g11	8V1	45.5	43.94	3.43
22	i1	8V2	68.5	65.94	3.73

Table 6.3 continued

S.No.	UT ID	Stock	Refinery measured viscosity at 210 ^{0}F (ssu)	Model Predictions (ssu)	Percent Deviation
23	i2	8V2	70.1	68.31	2.56
24	i3	8V2	67	61.85	7.68
25	i4	8V2	65.2	61.11	6.28
26	i5	8V2	70.2	67.93	3.23
27	i6	8V2	72.5	70.56	2.68
28	i7	8V2	66.2	62.35	5.81
29	i8	8V2	67.3	64.73	3.81
30	i9	8V2	63.7	59.56	6.50
31	i11	8V2	66.3	61.64	7.03
32	i12	8V2	71.6	69.15	3.42
33	i13	8V2	70.4	68.26	3.04
34	i14	8V2	71.2	66.25	6.95
35	i15	8V2	69.9	66.83	4.40
36	k1	8V3	97.1	92.12	5.13
37	k2	8V3	99.5	92.40	7.13
38	k3	8V3	93.1	89.39	3.99
39	k5	8V3	93.2	90 25	3.16
40	k6	8V3	93.5	91.48	2.16
41	k7	8V3	93.1	91.65	1.56
42	k8	8V3	89.2	88.55	0.73

Table 6.3 continued

S.No.	UT ID	Stock	Refinery measured viscosity at 210 ^{0}F (ssu)	Model Predictions (ssu)	Percent Deviation
43	k9	8V3	90	88.40	1.78
44	k10	8V3	91	88.01	3.28
45	k11	8V3	93.8	89.36	4.74
46	k12	8V3	94.4	90.24	4.40
47	k13	8V3	92.9	89.50	3.66
48	k14	8V3	96.4	92.51	4.04
49	n1	9V1	45.5	43.74	3.87
50	n2	9V1	45.6	43.47	4.67
51	n4	9V1	46.1	45.20	1.95
52	n5	9V1	46	43.87	4.63
53	n6	9V1	46.1	44.46	3.55
54	n7	9V1	45.9	43.91	4.34
55	p1	9V2	76.7	75.23	1.91
56	p2	9V2	76.6	75.62	1.28
57	p3	9V2	77.6	74.80	3.60
58	p4	9V2	77.1	74.19	3.77
59	p5	9V2	76.4	74.68	2.26

Table 6.4 Prediction of viscosity at 100 ^{0}F. The model is based on IR spectral data collected from 400μ cell in the original OSA-R analyzer. SEP value is 38.90.

S.No.	UT ID	Stock	Refinery measured viscosity at 100 ^{0}F (ssu)	Model predictions (ssu)	Percent Deviation
1	a1	7V2	159.4	164.92	-3.46
2	a2	7V2	216.9	218.97	-0.96
3	a3	7V2	208.5	219.48	-5.27
4	a4	7V2	212.6	210.69	0.90
5	a5	7V2	197.7	209.70	-6.07
6	a6	7V2	216.7	199.68	7.85
7	a7	7V2	207.7	235.33	-13.30
8	a8	7V2	213.3	232.02	-8.78
9	d1	7A4	115.7	229.55	-98.40
10	d2	7A4	117.2	224.85	-91.85
11	d3	7A4	112	225.34	-101.19
12	d4	7A4	144	257.72	-78.97
13	d5	7A4	130.7	241.92	-85.10
14	g1	8V1	195	204.26	-4.75
15	g3	8V1	185.6	197.10	-6.19

Table 6.4 continued

S.No.	UT ID	Stock	Refinery measured viscosity at 100 ^{0}F (ssu)	Model predictions (ssu)	Percent Deviation
16	g5	8V1	202.7	200.86	0.91
17	g6	8V1	200.9	196.54	2.17
18	g7	8V1	193.4	194.50	-0.57
19	g8	8V1	181.8	209.46	-15.22
20	n1	9V1	221.2	223.73	-1.15
21	n2	9V1	223.9	235.36	-5.12
22	n3	9V1	200.5	212.86	-6.16
23	n4	9V1	232.5	234.53	-0.87
24	n5	9V1	230.6	238.30	-3.34
25	n6	9V1	237.8	237.06	0.31
26	n7	9V1	236	242.81	-2.89
12	d4	7A4	144	257.72	-78.97
13	d5	7A4	130.7	241.92	-85.10
14	g1	8V1	195	204.26	-4.75
15	g3	8V1	185.6	197.10	-6.19

Figure 6.4 shows the IR spectra of a few representative samples obtained using the optical cell in the original OSA-R. The absorbance of most of the peaks in the region of 1700 to 500 cm^{-1} is above 1.0. At absorbance level greater than 1.0, less than 10% of the original light beam reaches the detector as can be derived from equation 4.8. At this level the detection limit of the detector is questionable. Also, the linearity of the Beer-Lambert law breaks down at high absorbance level. Hence, any peaks with greater absorbance than 1.0 are unsuitable for quantitative modeling.

The region between 1700 and 500 cm^{-1} is called the "fingerprint" region in the infrared because of the characteristic pattern found for individual molecular species in this region. This region contains the unique absorption specific to any given substance. The absorbance of most of the peaks in the region of 1700 to 500 cm^{-1} is above 1.0 as can be seen in figure 6.4 and hence, was not used in the calibration model. This is one possible reason why the predictions for V_{100} were unsatisfactory. To test this hypothesis, a set of experiments was devised to measure the spectra at reduced absorbance level. This translated to reducing the path length of the optical cell. The idea of reducing the absorbance by diluting the sample in some solvent was not considered because the intent of OSA-R approach was to keep the sample preparation time to a minimum.

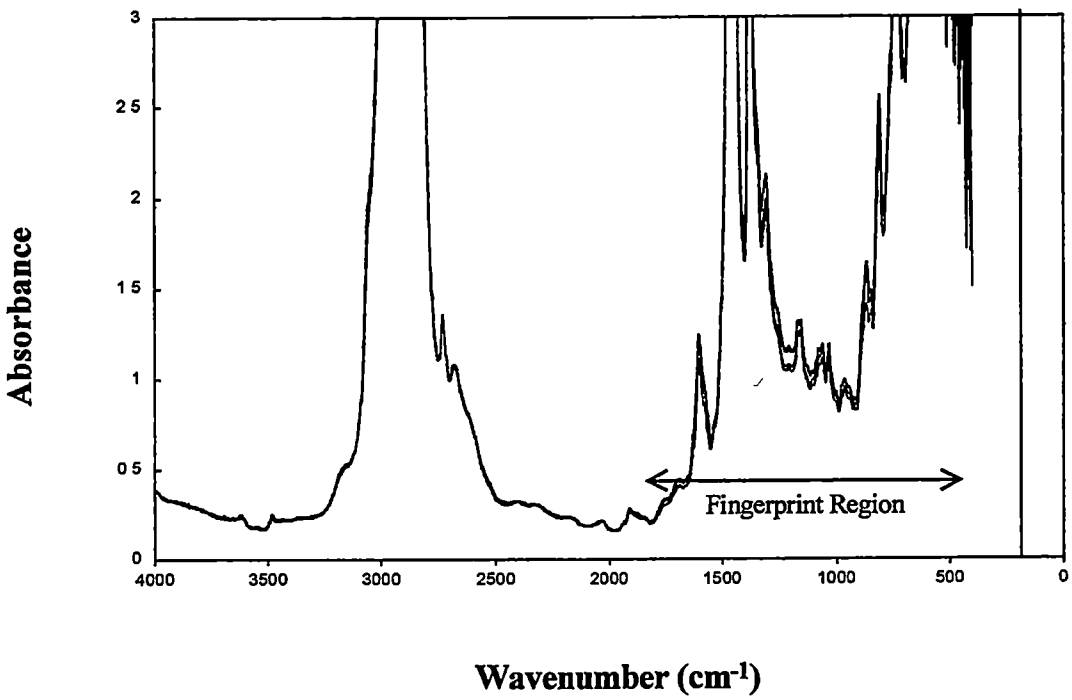


Figure 6.4 Infrared spectra of few of the representative samples obtained by OSA-R analyzer with the optical path-length as 400μ.

6.3.3 Modification in the Optical Cell of the OSA-R Analyzer

In the original OSA-R the path length of the optical cell was 400-microns. This optical cell was reduced to a path length of 100-microns. Reducing the path length of the cell added two complications to the measurement. First, because the samples were highly viscous, the reduced path length made it more difficult to flow oil through the cell. This increases the risk of cell damage and subsequent leakage during operation. Also, an optical effect known as "fringing" was observed. This effect adds a regular sinusoidal interference pattern to the recorded spectral data, which in turn adds error to the measurement. It is known that this optical characteristic originates from the nature of the cell windows (constructed from zinc selenide). This effect was in part subsequently over come by the use of especially coated windows (modified by an anti-reflection coating). The option of using a 100-micron cell on final prototype analyzer was never considered as an option because of the problems cited above. However, the experiment provided the opportunity to assess how the predictions would improve as more spectral peaks from the fingerprint region were used for modeling. New spectra of the samples were obtained with the new cell configuration and typical results are seen in Figure 6.5. It is noted that the spectral absorbance has decreased over the desired finger print region.

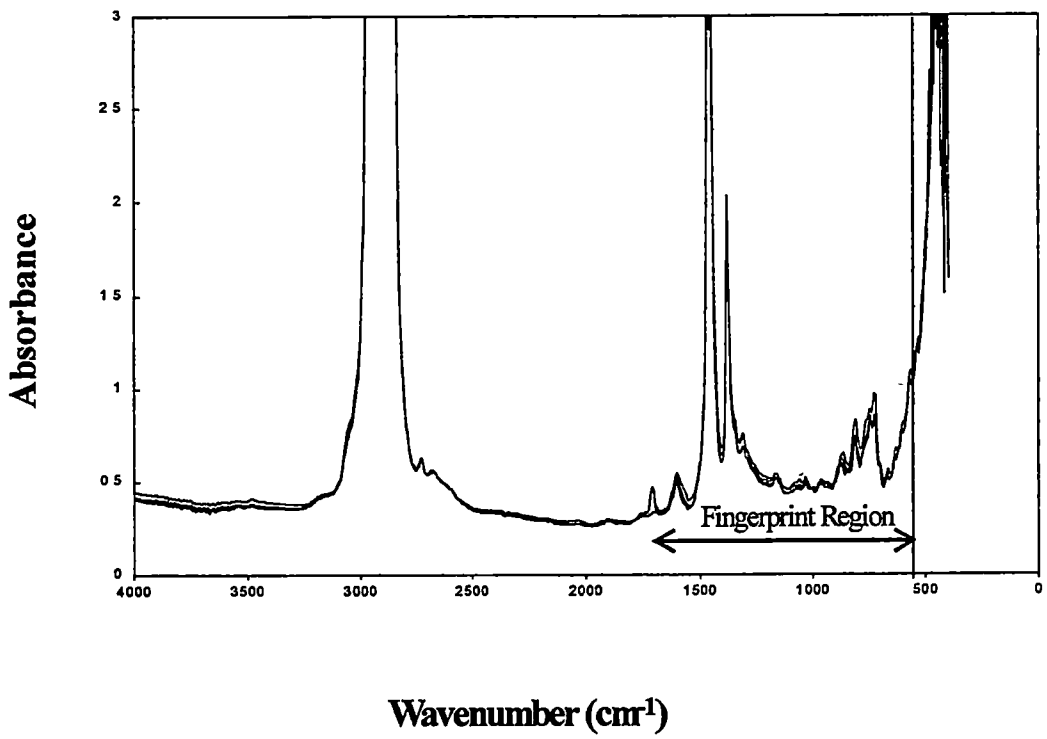


Figure 6.5 Infrared spectra of few of the representative samples obtained by OSA-R analyzer with the optical path-length as 100μ.

Unfortunately, there are still some regions (1500 to 1250 cm^{-1}) in the "finger print" zone where the absorbance are still too high for modeling.

The results of the new chemometric models based on spectral data collected from 100-micron optical cell can be seen Figure 6.6 and 6.7 and Table 6.5 and 6.6. The results show improvement over the original models, which were based on spectra obtained from the 400-micron optical cell. The predictions for V_{100} are still not totally acceptable but it is encouraging that a general trend is now observed, compared to the distorted data obtained from the 400-micron cell model, where most of the "finger print" region was neglected. It demonstrates the need to include more spectral information from the finger print region. This indicates that a reduction in the path length is desirable. However, because most of the heavy oil fractions are very viscous, an optical cell of reduced path length is expected to inhibit the flow of the samples through the cell. Thus, the option of using a thinner optical cell was not practical. Under these circumstances, the only option was to consider an alternative sampling technique. Attenuated Total Reflectance (ATR) is a well-established sampling technique that handles both problems of path length and sample flow. This technique has been described in chapter 4 and was utilized in the next phase of experiments.

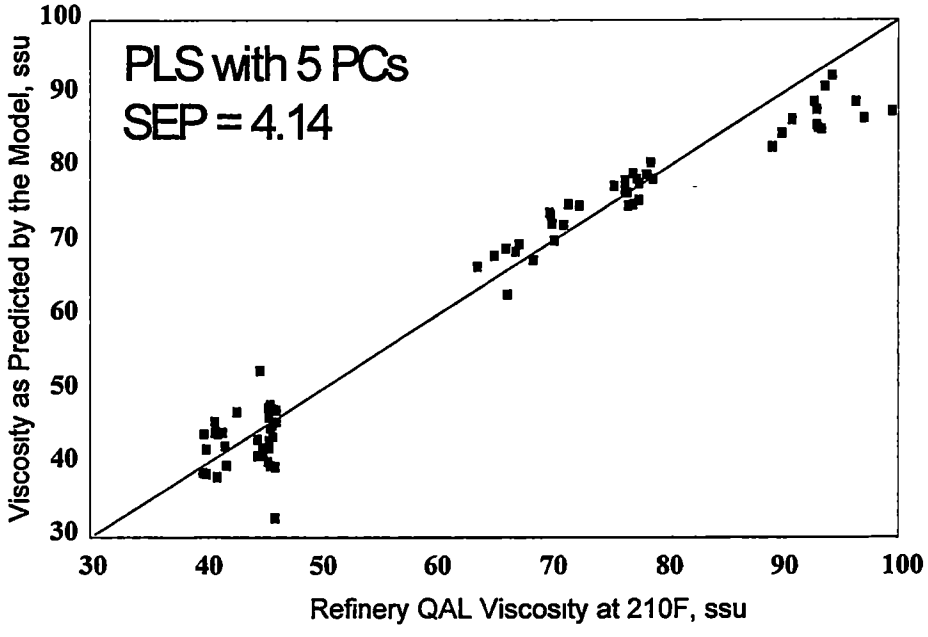


Figure 6.6 Partial Least Squares model for viscosity at 210 ^{0}F. Model is based on the infrared spectra obtained from OSA-R with the optical path-length of 100μ. 5 principal components were used and the SEP value was 4.14.

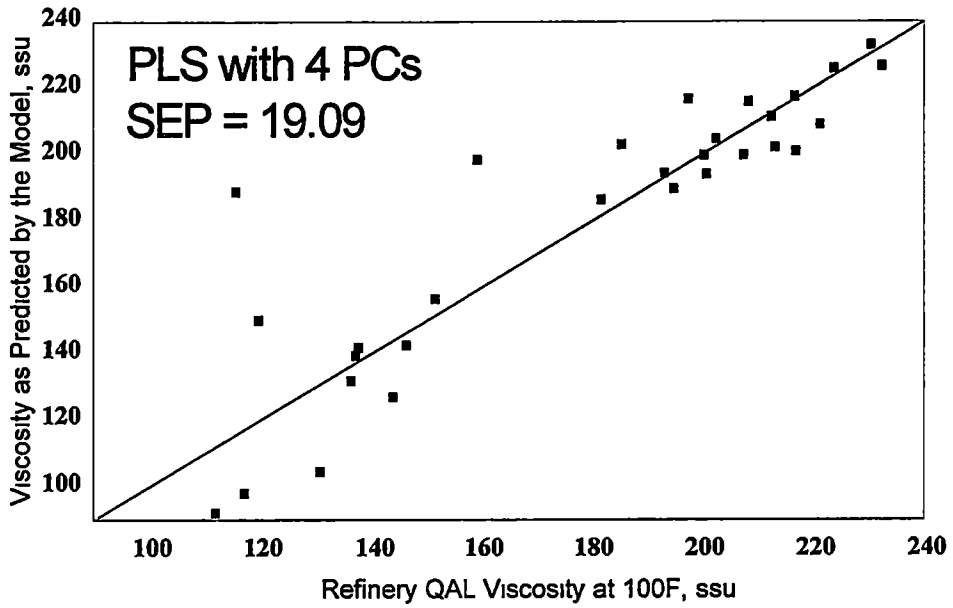


Figure 6.7 Partial Least Squares model for viscosity at 100 ^{0}F. Model is based on the infrared spectra obtained from OSA-R with the optical path-length of 100μ. 4 principal components were used and the SEP value was 19.09.

Table 6.5 Prediction of viscosity at 210 ^{0}F. The model is based on IR spectral data collected from 100μ cell in the modified OSA-R analyzer. SEP value is 4.14.

S.No.	UT ID	Stock	Refinery measured viscosity at 210 ^{0}F (ssu)	Model predictions (ssu)	Percent deviation
1	a1	7V2	42.7	45.91	-7.52
2	a2	7V2	46	44.72	2.77
3	a3	7V2	45.6	44.24	2.98
4	a4	7V2	45.8	45.60	0.44
5	a5	7V2	45	42.88	4.71
6	a6	7V2	46	40.31	12.36
7	a7	7V2	45.4	45.02	0.83
8	a8	7V2	45.6	45.23	0.81
9	d1	7A4	40	51.14	-27.86
10	d2	7A4	40	38.26	4.34
11	d3	7A4	39.7	33.87	14.69
12	d4	7A4	41.8	47.37	-13.33
13	d5	7A4	41	41.61	-1.50
14	g1	8V1	44.7	53.69	-20.11
15	g3	8V1	44.5	46.04	-3.47
16	g5	8V1	45.5	43.62	4.13
17	g6	8V1	45.4	43.95	3.19
18	g7	8V1	44.9	45.38	-1.07
19	g8	8V1	44.5	49.73	-11.75
20	g10	8V1	45.8	51.24	-11.88

Table 6.5 continued

S.No.	UT ID	Stock	Refinery measured viscosity at 210 ^{0}F (ssu)	Model predictions (ssu)	Percent deviation
21	g11	8V1	45.5	46.08	-1.27
22	i1	8V2	68.5	66.22	3.33
23	i2	8V2	70.1	68.76	1.91
24	i3	8V2	67	65.74	1.87
25	i4	8V2	65.2	64.19	1.55
26	i5	8V2	70.2	69.82	0.54
27	i6	8V2	72.5	73.58	-1.49
28	i7	8V2	66.2	62.64	5.38
29	i8	8V2	67.3	63.84	5.15
30	i9	8V2	63.7	64.79	-1.72
31	i11	8V2	66.3	68.45	-3.24
32	i12	8V2	71.6	77.32	-7.99
33	i13	8V2	70.4	75.93	-7.85
34	i14	8V2	71.2	69.80	1.97
35	i15	8V2	69.9	70.08	-0.26
36	k1	8V3	97.1	86.30	11.12
37	k2	8V3	99.5	89.44	10.11
38	k3	8V3	93.1	85.94	7.69
39	k5	8V3	93.2	83.85	10.04
40	k6	8V3	93.5	83.72	10.46

Table 6.5 continued

S.NO.	UT ID	Stock	Refinery measured viscosity at 210 ^{0}F (ssu)	Model predictions (ssu)	Percent deviation
41	k7	8V3	93.1	84.59	9.14
42	k8	8V3	89.2	83.24	6.69
43	k9	8V3	90	86.15	4.28
44	k10	8V3	91	84.71	6.91
45	k11	8V3	93.8	89.86	4.20
46	k12	8V3	94.4	94.12	0.30
47	k13	8V3	92.9	89.31	3.86
48	k14	8V3	96.4	94.39	2.09
49	n1	9V1	45.5	50.96	-12.00
50	n2	9V1	45.6	48.09	-5.47
51	n4	9V1	46.1	47.77	-3.61
52	n5	9V1	46	47.07	-2.32
53	n6	9V1	46.1	46.41	-0.68
54	n7	9V1	45.9	45.77	0.28
55	p1	9V2	76.7	77.03	-0.43
56	p2	9V2	76.6	79.33	-3.57
57	p3	9V2	77.6	80.05	-3.15
58	p4	9V2	77.1	78.19	-1.42
59	p5	9V2	76.4	80.20	-4.97
60	p7	9V2	77.6	78.88	-1.65

Table 6.5 continued

S.NO.	UT ID	Stock	Refinery measured viscosity at 210 ^{0}F (ssu)	Model predictions (ssu)	Percent deviation
61	p8	9V2	78.6	79.73	-1.43
62	p9	9V2	78.8	77.39	1.79
63	p10	9V2	77.4	77.17	0.30
64	p11	9V2	77.1	79.35	-2.92
65	p12	9V2	78.2	78.59	-0.49
66	p13	9V2	78.3	78.59	-0.36
67	p14	9V2	76.4	74.92	1.94
68	p15	9V2	75.5	76.36	-1.14
69	s1	9A5	39.8	41.29	-3.74
70	s2	9A5	40.8	41.01	-0.52
71	s3	9A5	40.8	42.93	-5.22
72	s4	9A5	40.9	39.70	2.94
73	s5	9A5	41.1	42.54	-3.50

Table 6.6 Prediction of viscosity at 100 ^{0}F. The model is based on IR spectral data collected from 100μ cell in the modified OSA-R analyzer. SEP value is 19.09.

S.No.	UT ID	Stock	Refinery measured viscosity at 100 ^{0}F (ssu)	Model predictions (ssu)	Percent deviation
1	a1	7V2	159.4	199.94	-25.43
2	a2	7V2	216.9	247.60	-14.15
3	a3	7V2	208.5	258.77	-24.11
4	a4	7V2	212.6	214.25	-0.77
5	a5	7V2	197.7	251.30	-27.11
6	a6	7V2	216.7	245.94	-13.49
7	a7	7V2	207.7	216.55	-4.26
8	a8	7V2	213.3	202.30	5.16
9	d1	7A4	115.7	182.70	-57.91
10	d2	7A4	117.2	119.90	-2.30
11	d3	7A4	112	116.37	-3.91
12	d4	7A4	144	140.01	2.77
13	d5	7A4	130.7	111.72	14.52
14	g1	8V1	195	187.65	3.77
15	g3	8V1	185.6	207.76	-11.94
16	g5	8V1	202.7	200.98	0.85
17	g6	8V1	200.9	189.85	5.50
18	g7	8V1	193.4	196.98	-1.85
19	g8	8V1	181.8	173.08	4.80
20	n1	9V1	221.2	217.52	1.67

Table 6.6 Continued

S.No.	UT ID	Stock	Refinery measured viscosity at 100 ^{0}F (ssu)	Model predictions (ssu)	Percent deviation
21	n2	9V1	223.9	223.45	0.20
22	n3	9V1	200.5	210.80	-5.14
23	n4	9V1	232.5	223.01	4.08
24	n5	9V1	230.6	235.84	-2.27
25	n6	9V1	237.8	242.25	-1.87
26	n7	9V1	236	254.87	-7.99
27	s1	9A5	119.7	138.14	-15.41
28	s2	9A5	137.8	141.76	-2.88
29	s3	9A5	137.4	144.86	-5.43
30	s4	9A5	136.5	132.83	2.69
31	s6	9A5	146.3	154.83	-5.83
32	s7	9A5	151.6	138.44	8.68

Near Infrared (NIR), spectroscopy was another available option. It has been used successfully for several refinery applications, in particular for the modeling of fuel oil properties [6,10]. Also, the spectral absorbance in the NIR region is much lower than that in mid-IR region. Thus, the problem of using long path length could be easily solved. However, the peaks in NIR are broad and overlapping, especially for samples like heavy oil composed of high molecular weight species with little structural variations. As a consequence the NIR spectra of different samples do not contain sufficient unique distinguishing features that can be used for determining the physical characteristics of the sample. This is in contrast to the higher information content available in the mid-IR spectra of the sample. The dark color of the samples might cause some interference to the NIR spectrum. For these reasons, NIR was not considered for modeling the properties of heavy oil fractions.

6.4 ATR IR Sampling Technique

The ATR IR technique requires a slightly different optical cell configuration than the transmission type of sampling used in the original OSA-R. Hence, experiments using ATR IR were conducted on a separate breadboard instrument rather than on the original OSA-R. The infrared spectrometer used was Impact 400 from Nicolet. This is the same spectrometer that was on the OSA-R analyzer. The

ATR optical cell used is depicted in Figure 6.8. It features a diamond prism with three reflections and a heated sampling surface. The use of this cell presented the following advantages:

- A diamond prism is inert, rugged and durable and hence, can be easily used in industrial environment. The cell geometry can be modified for on-line applications.
- The overall intensity of the recorded system was reduced to absorbance less than 1.0. This makes the entire finger print region available for modeling.
- The effective path length of the ATR increases with wavelength. As previously noted, the longer wavelength region contains information about the chain length of the hydrocarbons and hence, this enhancement is advantageous for the present application.
- A heated sampling surface ensures that the sample is maintained as a liquid.

6.4.1 Modeling of Viscosity Parameters

A fresh set of spectra was obtained with the ATR IR cell and new chemometric models were built based on these spectra. It can see in Figure 6.9 that the ATR IR spectra have absorbance levels lower than 1.0, thus allowing us to use the entire spectral information (excluding the spectral artifact in the region 2500 to 1800 cm^{-1}) for modeling purposes. The spectral artifacts in the region 2500 to 1800

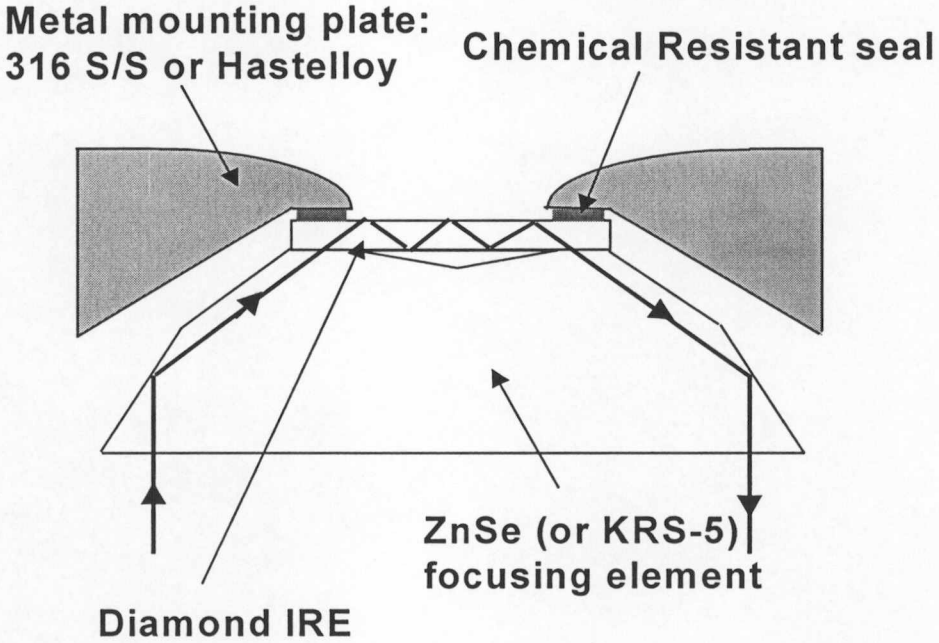


Figure 6.8 Schematic of the Attenuated Total Reflectance (ATR) cell used for sampling.

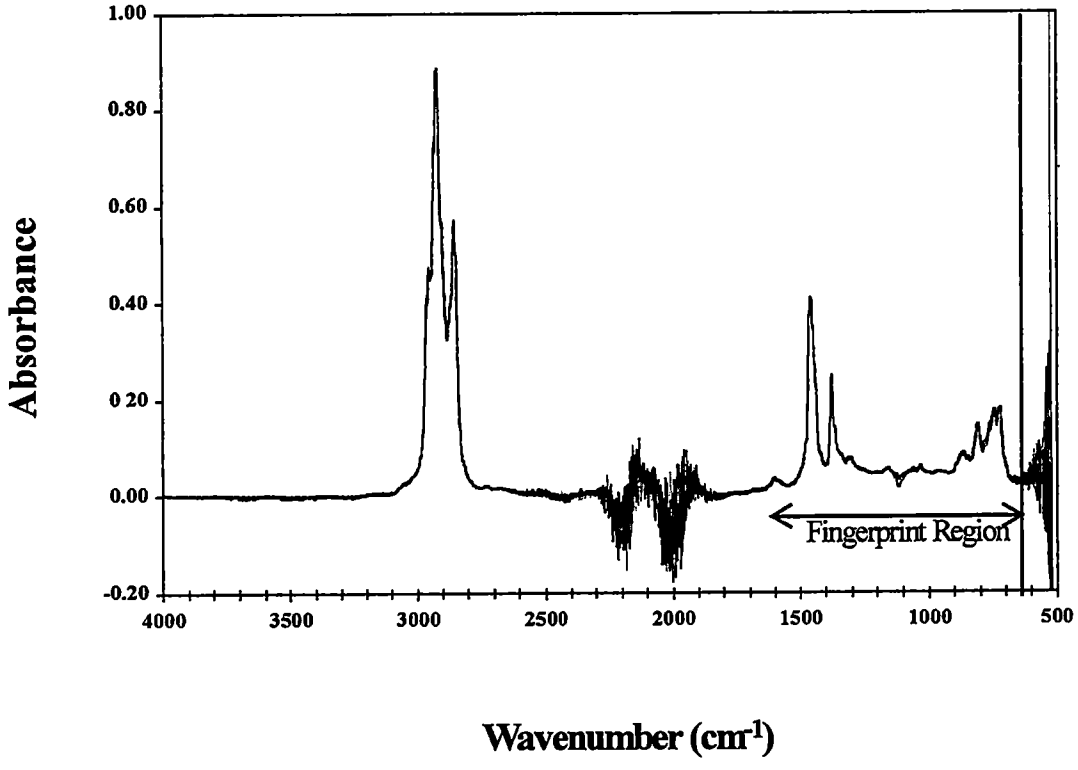


Figure 6.9 Infrared spectra of few representative sample obtained by the ATR sampling technique.

cm^{-1} are attributed to the absorption by the diamond prism. In effect, the entire "finger print" region is available for modeling.

The results from the new models based on ATR IR type spectra show significant improvement over the original models as can be seen in Figure 6.10 and 6.11 and Table 6.7 and 6.8. The predictions of both V_{100} and V_{210} are within 5 % of the actual values and the SEP values are 1.64 and 3.34 respectively.

The trend in the results (from a 400-micron cell to a 100-micron and then on to an ATR IR type cell) gives us an insight that the finger print region of the IR spectra contains important information that correlates to the physical properties of the heavy oil fractions. In the present example, it is demonstrated that as we incorporate more spectral information from the finger print region into our models, the prediction of the models is improved.

Encouraged by the good results obtained from the new models for V_{100} and V_{210}, chemometric models were built for the prediction of the Viscosity Index (VI). The predictions of models based on ATR IR spectral information were within 5% of the actual values (Figure 6.12 and Table 6.9) thus reconfirming the fact that the "finger print" region of the IR spectra contains important information regarding the physical properties of the heavy oil fractions.

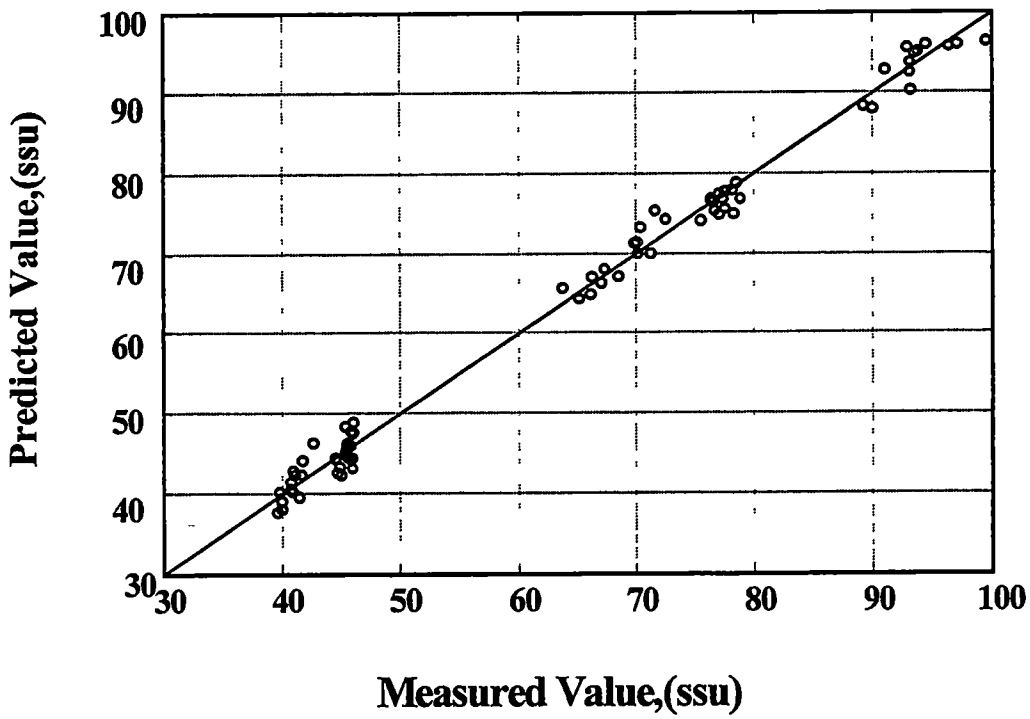


Figure 6.10 Predictive model for viscosity at 210 ^{0}F. The model is based on the infrared spectra obtained by ATR sampling technique. Partial Least Squares with 5 principal component was used and the SEP value is 1.64.

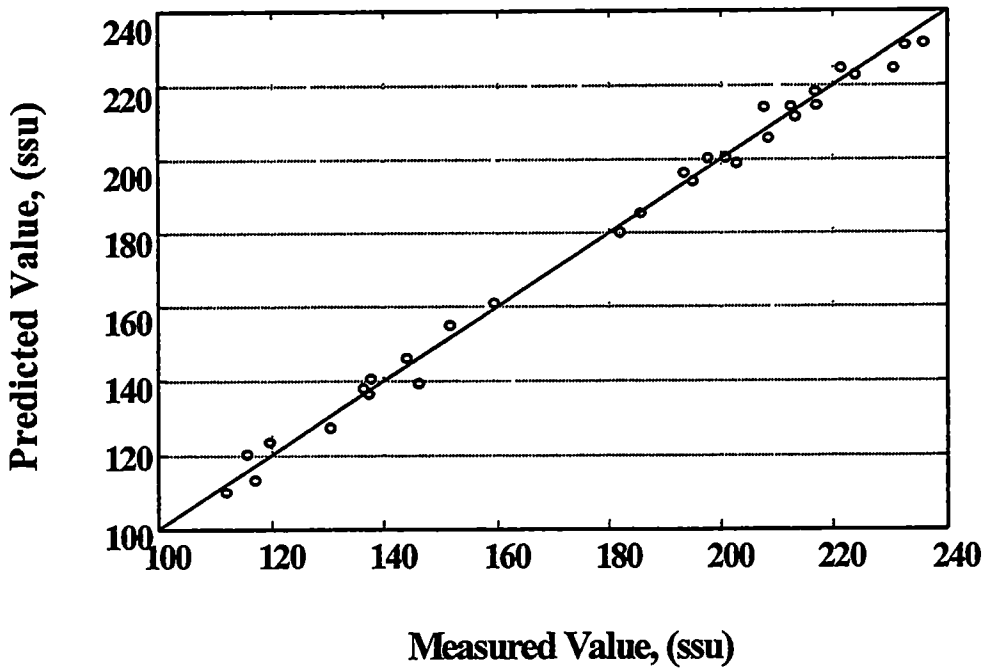


Figure 6.11 Predictive model for viscosity at 100 ^{0}F. The model is based on the infrared spectra obtained by ATR sampling technique. Partial Least Squares with 6 principal components were used and the SEP value is 3.34.

Table 6.7 Prediction of viscosity at 210 ^{0}F. The model is based on IR spectral data collected using ATR sampling technique. SEP value is 1.64.

S.No.	UT ID	Stock	Refinery measured viscosity at 210 ^{0}F (ssu)	Model predictions (ssu)	Percent deviation
1	a1	7V2	42.7	46.29	8.40
2	a2	7V2	46	44.46	3.35
3	a3	7V2	45.6	44.56	2.27
4	a4	7V2	45.8	44.38	3.11
5	a5	7V2	45	42.38	5.82
6	a6	7V2	46	43.19	6.12
7	a7	7V2	45.4	48.48	6.78
8	a8	7V2	45.6	46.38	1.72
9	d1	7A4	40	38.18	4.54
10	d2	7A4	40	39.13	2.17
11	d3	7A4	39.7	37.77	4.85
12	d4	7A4	41.8	44.27	5.91
13	d5	7A4	41	42.89	4.61
14	g1	8V1	44.7	42.76	4.33
15	g3	8V1	44.5	44.40	0.22
16	g5	8V1	45.5	45.44	0.13
17	g6	8V1	45.4	45.22	0.41
18	g7	8V1	44.9	43.39	3.35
19	g8	8V1	44.5	44.45	0.11
20	g10	8V1	45.8	46.03	0.51

Table 6.7 Continued

S.No.	UT ID	Stock	Refinery measured viscosity at 210 ^{0}F (ssu)	Model predictions (ssu)	Percent deviation
21	g11	8V1	45.5	44.89	1.34
22	i1	8V2	68.5	67.23	1.86
23	i2	8V2	70.1	71.45	1.92
24	i3	8V2	67	66.32	1.02
25	i4	8V2	65.2	64.38	1.26
26	i5	8V2	70.2	70.13	0.10
27	i6	8V2	72.5	74.27	2.45
28	i7	8V2	66.2	64.87	2.00
29	i8	8V2	67.3	68.09	1.17
30	i9	8V2	63.7	65.78	3.27
31	i11	8V2	66.3	67.09	1.19
32	ı12	8V2	71.6	75.35	5.24
33	i13	8V2	70.4	73.34	4.18
34	i14	8V2	71.2	70.13	1.50
35	i15	8V2	69.9	71.26	1.94
36	k1	8V3	97.1	96.06	1.07
37	k2	8V3	99.5	96.44	3.08
38	k3	8V3	93.1	92.53	0.61
39	k5	8V3	93.2	90.31	3.10
40	k6	8V3	93.5	94.98	1.59

Table 6.7 continued

S.No.	UT ID	Stock	Refinery measured viscosity at 210 ^{0}F (ssu)	Model predictions (ssu)	Percent deviation
41	k7	8V3	93.1	93.86	0.82
42	k8	8V3	89.2	88.32	0.99
43	k9	8V3	90	87.95	2.28
44	k10	8V3	91	92.82	2.00
45	k11	8V3	93.8	95.21	1.50
46	k12	8V3	94.4	96.01	1.70
47	k13	8V3	92.9	95.66	2.97
48	k14	8V3	96.4	95.73	0.69
49	n1	9V1	45.5	45.99	1.09
50	n2	9V1	45.6	46.16	1.24
51	n4	9V1	46.1	48.90	6.07
52	n5	9V1	46	47.53	3.34
53	n6	9V1	46.1	47.64	3.35
54	n7	9V1	45.9	47.87	4.29
55	p1	9V2	76.7	75.41	1.69
56	p2	9V2	76.6	76.47	0.17
57	p3	9V2	77.6	77.71	0.14
58	p4	9V2	77.1	74.91	2.85
59	p5	9V2	76.4	76.91	0.67
60	p7	9V2	77.6	75.69	2.46

Table 6.7 continued

S.No.	UT ID	Stock	Refinery measured viscosity at 210 ^{0}F (ssu)	Model predictions (ssu)	Percent deviation
61	p8	9V2	78.6	78.87	0.34
62	p9	9V2	78.8	76.88	2.43
63	p10	9V2	77.4	76.84	0.72
64	p11	9V2	77.1	77.48	0.49
65	p12	9V2	78.2	78.03	0.21
66	p13	9V2	78.3	74.96	4.27
67	p14	9V2	76.4	76.68	0.37
68	p15	9V2	75.5	74.17	1.76
69	s1	9A5	39.8	40.31	1.28
70	s2	9A5	40.8	41.51	1.75
71	s3	9A5	40.8	40.68	0.30
72	s4	9A5	40.9	40.22	1.67
73	s5	9A5	41.1	42.34	3.02
74	s6	9A5	41.47	39.68	4.33
75	s7	9A5	41.7	42.38	1.63

Table 6.8 Prediction of viscosity at 100 ^{0}F. The model is based on IR spectral data collected using ATR sampling technique. SEP value is 3.34.

S.No.	UT ID	Stock	Refinery measured viscosity at 100 ^{0}F (ssu)	Model predictions (ssu)	Percent deviation
1	a1	7V2	159.4	161.21	1.13
2	a2	7V2	216.9	214.55	1.08
3	a3	7V2	208.5	205.65	1.37
4	a4	7V2	212.6	214.29	0.79
5	a5	7V2	197.7	200.13	1.23
6	a6	7V2	216.7	218.21	0.70
7	a7	7V2	207.7	214.11	3.08
8	a8	7V2	213.3	211.57	0.81
9	d1	7A4	115.7	120.34	4.01
10	d2	7A4	117.2	113.32	3.31
11	d3	7A4	112	110.18	1.62
12	d4	7A4	144	146.35	1.63
13	d5	7A4	130.7	127.47	2.47
14	g1	8V1	195	193.94	0.54
15	g3	8V1	185.6	185.38	0.12
16	g5	8V1	202.7	198.99	1.83
17	g6	8V1	200.9	200.50	0.20
18	g7	8V1	193.4	196.27	1.48
19	g8	8V1	181.8	180.04	0.97
20	n1	9V1	221.2	224.48	1.48

Table 6.8 Continued

S.No.	UT ID	Stock	Refinery measured viscosity at 100 ^{0}F (ssu)	Model predictions (ssu)	Percent deviation
21	n2	9V1	223.9	222.71	0.53
22	n4	9V1	232.5	230.66	0.79
23	n5	9V1	230.6	224.45	2.67
24	n6	9V1	237.8	243.76	2.51
25	n7	9V1	236	231.30	1.99
26	s1	9A5	119.7	123.50	3.17
27	s2	9A5	137.8	140.64	2.06
28	s3	9A5	137.4	136.36	0.76
29	s4	9A5	136.5	138.17	1.22
30	s6	9A5	146.3	139.37	4.74
31	s7	9A5	151.6	155.21	2.38

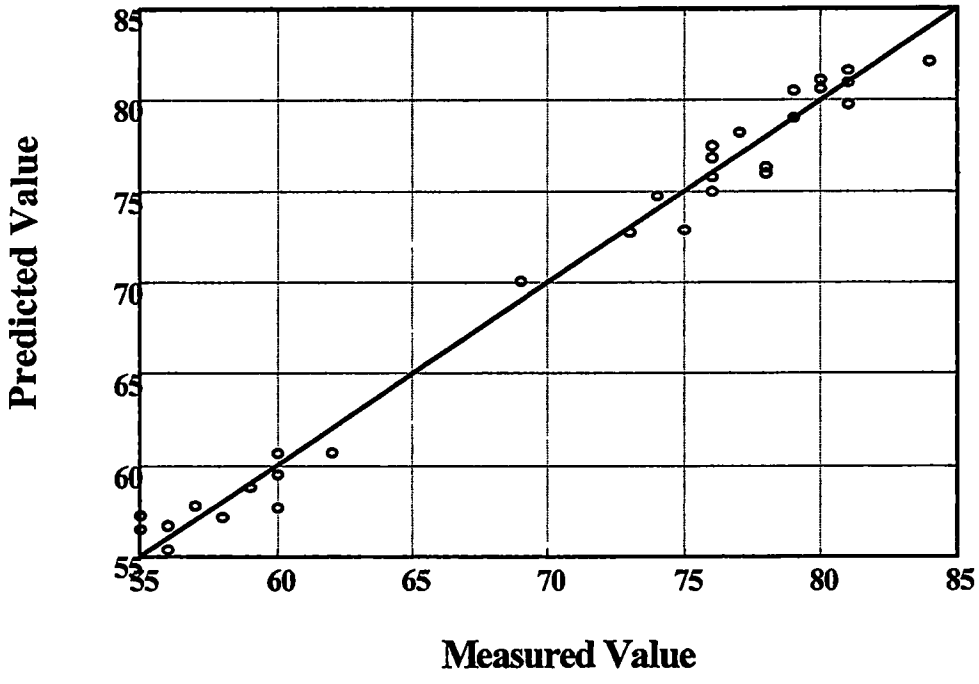


Figure 6.12 Predictive model for viscosity index. The model is based on the infrared spectra obtained by ATR sampling technique. Partial Least Squares was used with 6 principal components and the SEP value was 1.36.

Table 6.9 Prediction of viscosity index. The model is based on the IR spectral data collected using ATR sampling technique. SEP value is 1.36.

S.No.	UT ID	Stock	Refinery measured viscosity index	Model predictions	Percent deviation
1	a1	7V2	69	70	1.53
2	a2	7V2	74	75	0.94
3	a3	7V2	76	75	1.31
4	a4	7V2	76	77	1.08
5	a5	7V2	75	73	2.83
6	a6	7V2	76	77	1.91
7	a7	7V2	73	73	0.35
8	d1	7A4	79	79	0.00
9	d2	7A4	77	78	1.56
10	d3	7A4	78	76	2.57
11	d4	7A4	76	76	0.26
12	d5	7A4	78	76	2.15
13	g1	8V1	81	80	1.56
14	g3	8V1	79	80	1.86
15	g5	8V1	80	81	1.26
16	g6	8V1	81	82	0.72
17	g7	8V1	80	81	1.34
18	g8	8V1	84	82	2.26
19	g10	8V1	80	81	0.77
20	g11	8V1	81	81	0.04

Table 6.9 Continued

S.No.	UT ID	Stock	Refinery measured viscosity index	Model predictions	Percent deviation
21	n1	9V1	62	61	2.10
22	n2	9V1	60	61	1.10
23	n4	9V1	60	60	0.81
24	n5	9V1	59	59	0.35
25	n6	9V1	56	55	1.10
26	n7	9V1	55	55	0.65
27	s1	9A5	56	57	1.26
28	s2	9A5	56	57	1.20
29	s3	9A5	55	57	4.11
30	s4	9A5	58	57	1.43
31	s5	9A5	55	56	2.66
32	s6	9A5	60	58	3.86
33	s7	9A5	57	58	1.45

6.4.2 Compositional Property Correlation

In addition to the measurement of the physical properties, knowledge of the chemical composition of hydrocarbon fractions is important in refinery production. Existing methods for characterizing the composition in refinery labs are referenced earlier in chapter 2. These are not particularly convenient or appropriate for "real-time" process control or process monitoring. Infrared spectroscopy does offer the potential for making these measurements, by the use of chemometric modeling. One issue, however, is the need to obtain a set of well-characterized samples. Laboratory techniques such as nuclear magnetic resonance have been established as being suitable for this characterization. NMR can provide detailed compositional information about the sample. Carbon-13 (^{13}C) and proton (^{1}H) NMR spectra have been used extensively for obtaining the composition of oil fractions and these results compare well with the standard ASTM D2140 procedure for obtaining the relative composition in terms of the percentages of the PNA (Paraffins, Naphthenes, Aromatics) [72]. In this phase of the project, the primary analysis of the samples for relative compositional content was achieved by nuclear magnetic resonance spectroscopy.

Though NMR has been extensively used to establish the compositional properties of crude oils [67,73], it cannot be used directly in the instrumentation of a prototype analyzer meant for on-site applications. This is because NMR is a big laboratory based technique and in general is inappropriate for process instrumentation; sample preparation is cumbersome, and long data acquisition times are required, and a controlled environment is necessary for reliable operation of the instrument. These facts make it impossible to use ^{13}C NMR for rapid on-line determination of the compositional properties. Bearing in mind that the physical properties (V100, V210, and VI) are directly influenced by the composition and correlated well with the ATR IR spectral data, it was believed that it would also correlate well with the compositional characteristics derived from NMR experiments. An attempt was made to establish a correlation of ATR IR spectral information to the compositional characteristic data obtained from ^{13}C NMR experiments.

Varian Gemini-2000 NMR was used to obtain the NMR data. The NMR operated at 300 MHz and deutero-chloroform was used as solvent. The experimental parameters for ^{13}C NMR was: pulse width, 9μs (45^0); data points, 68096; and number of scans, 200. The experimental parameters used for ^{1}H NMR was: pulse width, 2μs (45^0); data points, 17984; and number of scans, 20. Once the spectra of the selected sample set were obtained, the relative percentages were determined. The

relative composition of the sample is determined from the ^{13}C NMR spectrum as follows:

Aromatic: area between 110 and 140 ppm

Naphthenic: area between 25 and 45 ppm

Paraffinic: area between 5 and 25 ppm and 45 and 60 ppm [42].

Proton NMR of the samples was also obtained but at present they were not used for modeling. Proton NMR data would be useful if we want further compositional details such as percentages of iso-paraffinic, olefinic etc.

Once the samples were characterized, the next step was to correlate the compositional parameter data obtained from the ^{13}C NMR study to the ATR IR spectra by the use of chemometric modeling. The predictions of these models were good and can be seen in Figure 6.13 to 6.15 and Tables 6.10 to 6.12.

6.5 Characterization of Oil Color

As described in section 2.2.6, the standard color measurement technique is very subjective and hence, color of the product has limited use in process control. At the same time the consumer can readily observe the color of the products and hence, make subjective judgement about product quality. Bearing this in mind, it is

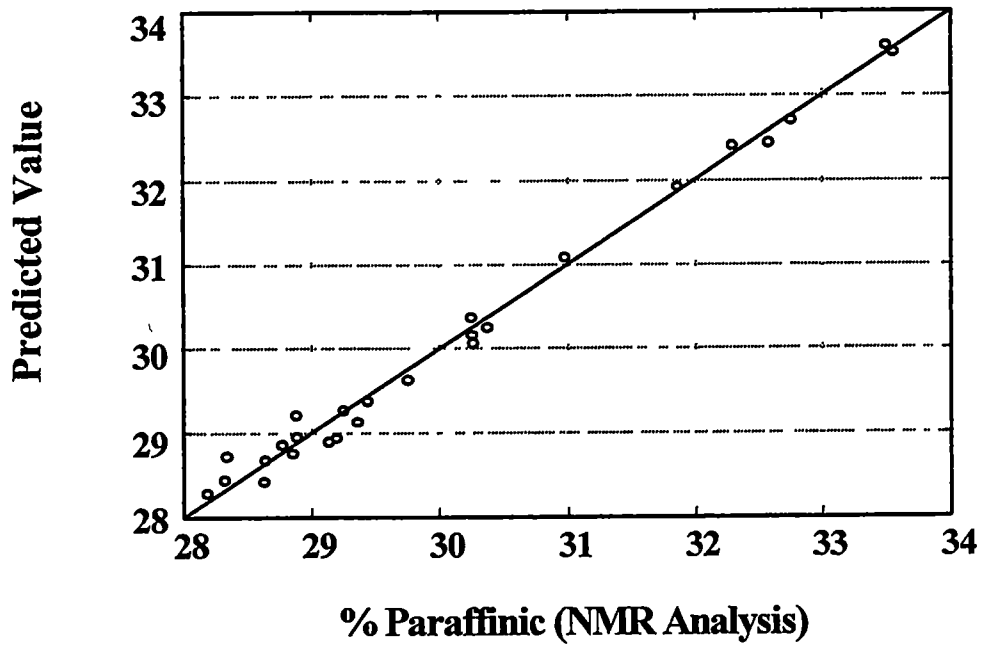


Figure 6.13 Predictive model for paraffinic composition in the samples. Model correlating the percentage paraffinic content in the samples to the infrared spectra of the samples obtained using ATR sampling technique. Partial Least Squares with 6 principal components was used for modeling. The SEP value is 1.15.

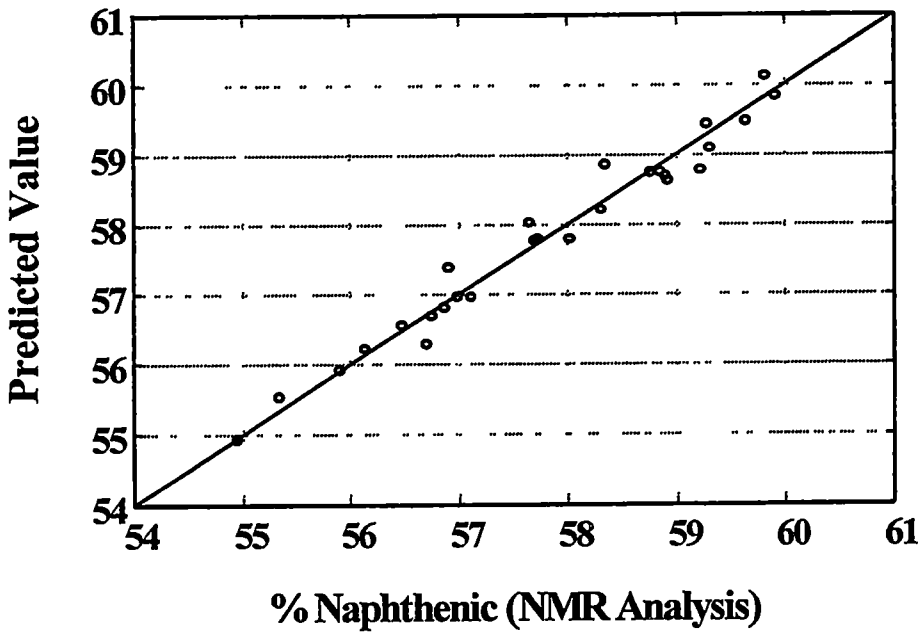


Figure 6.14 Predictive model for naphthenic composition in the samples. Model correlating the percentage naphthenic content in the samples to the infrared spectra of the samples obtained using ATR sampling technique. Partial Least Squares with 6 principal components was used for modeling. The SEP value is 1.28.

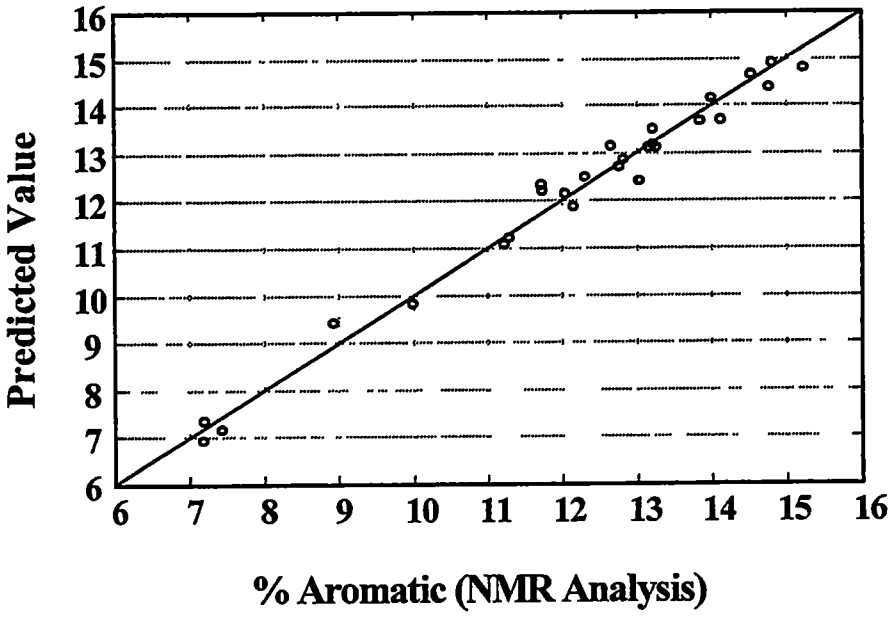


Figure 6.15 Predictive model for aromatic composition in the samples. Model correlating the percentage aromatic content in the samples to the infrared spectra of the samples obtained using ATR sampling technique. Partial Least Squares with 6 principal components was used for modeling. The SEP value is 1.61.

Table 6.10 Prediction of relative paraffinic content. Model was built by correlating the IR spectral data collected by ATR technique to the ^{13}C NMR primary analysis results. SEP value is 1.15.

S.No.	Sample	% Paraffinic content by ^{13}C NMR analysis	Model prediction	Percent deviation
1	a1	29.139	28.9051	0.80
2	a4	28.875	29.2181	1.19
3	a6	29.255	29.2706	0.05
4	a8	30.254	30.0622	0.63
5	d1	30.242	30.3781	0.45
6	d3	30.972	31.0849	0.36
7	d5	30.368	30.2557	0.37
8	g3	30.252	30.1643	0.29
9	g5	28.773	28.8659	0.32
10	g8	29.44	29.3752	0.22
11	i1	28.182	28.287	0.37
12	i2	29.752	29.6289	0.41
13	i4	28.852	28.7597	0.32
14	i6	28.321	28.4449	0.44
15	i7	29.361	29.1378	0.76

Table 6.10 Continued

S.No.	Sample	% Paraffinic content by ^{13}C NMR analysis	Model prediction	Percent deviation
16	i9	29.199	28.947	0.86
17	k2	28.333	28.7333	1.41
18	k3	28.767	28.8576	0.31
19	k8	28.883	28.9549	0.25
20	k10	28.635	28.6793	0.15
21	k12	28.63	28.4243	0.72
22	n1	31.863	31.9273	0.20
23	n4	32.577	32.4382	0.43
24	n6	32.294	32.4058	0.35
25	s1	32.751	32.7033	0.15
26	s5	33.49	33.5845	0.28
27	s7	33.545	33.5109	0.10

Table 6.11 Prediction of relative naphthenic content. Model was built by correlating the IR spectral data collected by ATR technique to the ^{13}C NMR primary analysis results. SEP value is 1.28.

S.No.	Sample	% Naphthenic content by ^{13}C NMR analysis	Model prediction	Percent deviation
1	a1	57.648	58.0298	0.66
2	a4	59.907	59.8316	0.13
3	a6	56.749	56.6929	0.10
4	a8	54.949	54.9291	0.04
5	d1	57.106	56.9707	0.24
6	d3	56.871	56.8238	0.08
7	d5	56.472	56.5558	0.15
8	g3	55.899	55.9213	0.04
9	g5	56.696	56.288	0.72
10	g8	55.333	55.5283	0.35
11	i1	57.699	57.7742	0.13
12	i2	56.987	56.9668	0.04
13	i4	58.841	58.757	0.14
14	i6	58.914	58.6412	0.46
15	i7	58.897	58.7023	0.33

Table 6.11 Continued

S.No.	Sample	% Naphthenic content by ^{13}C NMR analysis	Model prediction	Percent deviation
16	i9	58.756	58.7451	0.02
17	k2	56.905	57.387	0.85
18	k3	58.019	57.7925	0.39
19	k8	58.298	58.2201	0.13
20	k10	58.334	58.8624	0.91
21	k12	59.638	59.4821	0.26
22	n1	59.217	58.7882	0.72
23	n4	56.131	56.222	0.16
24	n6	57.72	57.7984	0.14
25	s1	59.813	60.1272	0.53
26	s5	59.307	59.0971	0.35
27	s7	59.272	59.4432	0.29

Table 6.12 Prediction of relative aromatic content. Model was built by correlating the IR spectral data collected by ATR technique to the ^{13}C NMR primary analysis results. SEP value is 1.61.

S.No.	Sample	% Aromatics content by ^{13}C NMR analysis	Model prediction	Percent deviation
1	a1	13.212	13.196	0.12
2	a4	11.219	11.093	1.12
3	a6	13.996	14.169	1.24
4	a8	14.797	14.909	0.76
5	d1	12.652	13.156	3.98
6	d3	12.157	11.885	2.23
7	d5	13.16	13.113	0.35
8	g3	13.848	13.690	1.13
9	g5	14.528	14.662	0.92
10	g8	15.227	14.798	2.81
11	i1	14.12	13.701	2.96
12	i2	13.261	13.121	1.05
13	i4	12.307	12.497	1.54
14	i6	12.764	12.712	0.40
15	i7	11.741	12.227	4.15

Table 6.12 Continued

S.No.	Sample	% Aromatics content by ^{13}C NMR analysis	Model prediction	Percent deviation
16	i9	12.044	12.154	0.92
17	k2	14.761	14.397	2.46
18	k3	13.214	13.516	2.29
19	k8	12.819	12.873	0.43
20	k10	13.031	12.415	4.73
21	k12	11.731	12.356	5.29
22	n1	8.919	9.428	5.71
23	n4	11.291	11.223	0.60
24	n6	9.988	9.838	1.50
25	s1	7.435	7.172	3.54
26	s5	7.203	7.355	2.12
27	s7	7.183	6.945	3.31

important to develop a reliable technique for the characterization of the color of refined lube oils.

Color of the petroleum fractions comes from aromatics and asphaltenes containing components. The concentration of these species in heavy fractions is relatively low, thus making it impractical to use FTIR for the measurement of color. Color characterization based on visible spectroscopy was conceived to be a reliable technique since visible spectral data are directly related to the color.

Ultraviolet (UV)/visible spectroscopy was used in the current work for characterizing the color. The light source was an Ocean Optics tungsten halogen lamp with the spectral output of 370 nanometers to 2 microns. The detector is an array of 2048 elements CCD detector. The sample holder was heated to ensure that the sample remained liquid and did not solidify during the process of spectral collection. The UV/visible spectra of a few representative samples can be seen in Figure 6.16. Sample "k14" is the darkest while sample "s1" is the lightest. Sample "a2' & "i2" have intermediate color. The trend of the spectra reaffirms the gradation in the color of the samples and so models built on the UV/visible spectra can be expected provide good correlation.

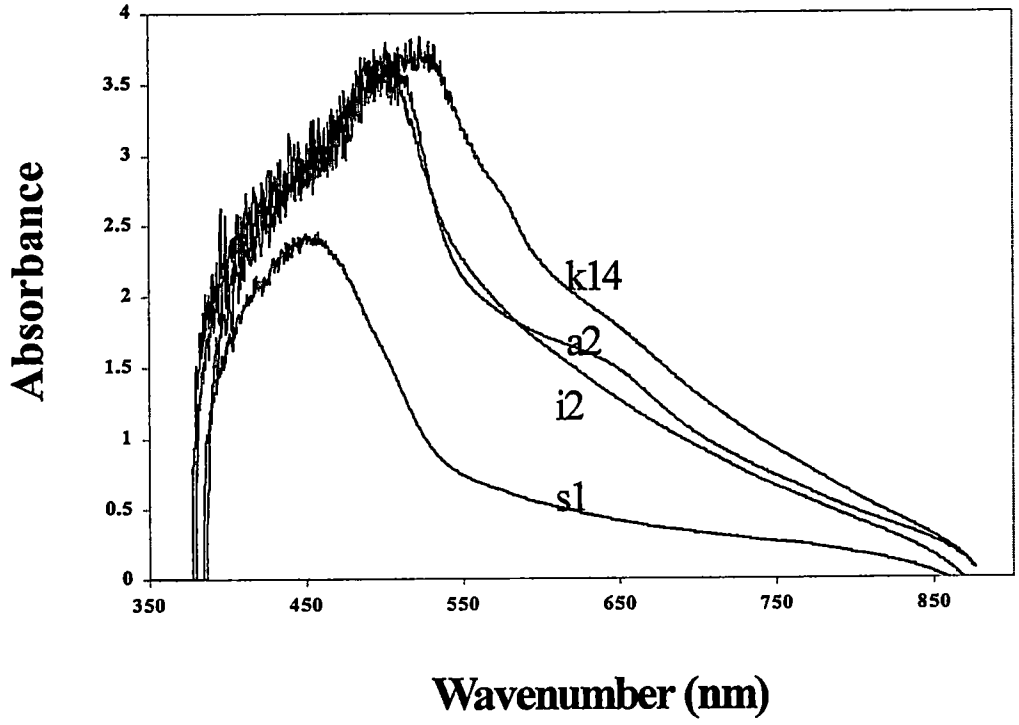


Figure 6.16 Visible spectra of few of the representative samples.

The UV/visible spectra of the samples were modeled against the color values provided by Top Source. The color values were obtained by the standard ASTM D1500 method discussed in chapter2. The result can be seen in Figure 6.17 and Table 6.13. The predicted values show deviations (around 10%) from the actual result. A systematic grouping of the data into two clusters with a bias offset can be seen in Figure 6.17. This shows that the predictions are not random. The samples are, on an average 3 years old and are expected to have darkened. Consequently, the color values provided by Top Source might be inaccurate and are likely to be the cause of the deviations seen in our results.

Software is available that directly measures tri-stimulus values of the sample based on its UV/visible spectra. The tri-stimulus standard defines the color of a sample in terms of three numbers rather than a single number. These three numbers are a representation of the respective intensity of the red, green and blue color whose combination can reproduce the original color of that sample. Although this type of analysis is presently not used in the petroleum industry for color characterization, it is expected to be more accurate for on-line predictions.

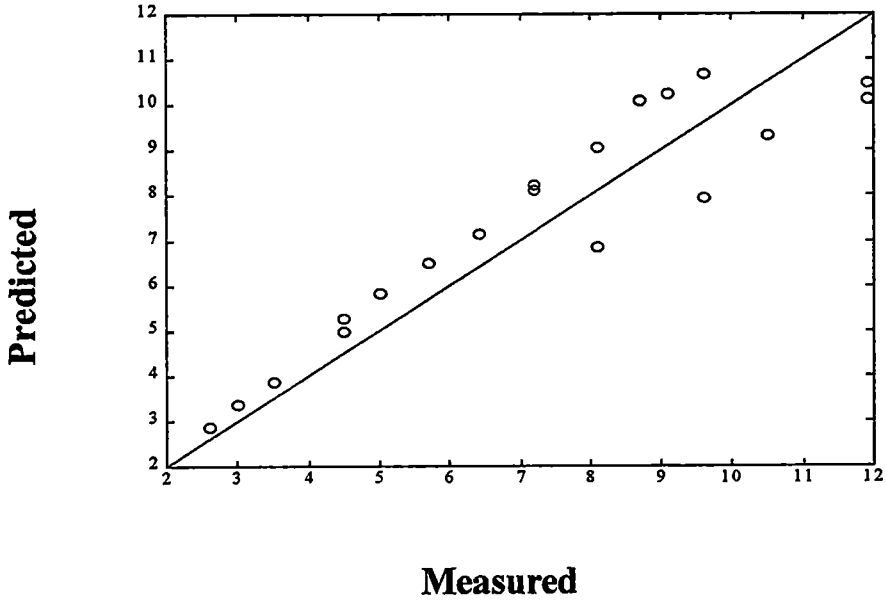


Figure 6.17 Partial Least Squares predictive model for the color of the samples. The model is based on the visible spectra of the samples. 5 principal components were used and the SEP value is 5.67.

Table 6.13 Prediction of the color of the sample. Model is based on the visible spectra of the samples. SEP value is 5.67.

S.No.	Sample	Refinery measured values of the color	Model prediction	Percent deviation
1	a2	9.1	10.25	12.66
2	d4	10.5	9.33	-11.13
3	g5	11.1	12.67	14.10
4	g7	11.9	10.11	-15.04
5	i1	9.6	10.68	11.24
6	i2	8.1	9.08	12.08
7	i6	8.7	10.11	16.15
8	i12	7.2	8.14	13.04
9	k1	3.5	3.88	10.72
10	k2	2.6	2.87	10.35
11	k8	4.5	5.00	11.13
12	k14	3	3.39	13.04
13	n2	9.6	7.95	-17.14
14	p1	7.2	8.24	14.46
15	p5	8.1	6.86	-15.33
16	p7	6.4	7.17	12.02
17	p9	5	5.84	16.85
18	p10	5.7	6.52	14.39
19	p13	4.5	5.27	17.13
20	s1	11.9	10.48	-11.91
21	s6	10.5	9.32	-11.26

Color characterization is generally used to determine the contamination level in the oil but another important commercial application of this technology is in the production of white oils used for FDA approved medicinal and food products.

Chapter 7

Conclusions and Future Work

In section 2.1, it was discussed that the characterization of heavy oil is important for production process and quality control. The existing conventional methods for such characterization are labor intensive. Furthermore, they cannot be used conveniently for on-line characterization. Optical spectrometric methods on the other hand are fast and easy to adapt for on-line measurements. Also, results from these spectrometric methods are comparable to the standard ASTM methods now in use. Hence, an instrument based on optical characterization of heavy oil fractions would improve the process and quality control in the refining of these products. In addition, there is associated time and cost saving benefits thereby, increasing the return on capital investment.

The results and conclusion from the experiments conducted during the course of this work are as follows:

- The original OSA-R was inappropriate for refining applications. The predictions of the key oil parameters (Viscosity, VI & color) from the OSA-R were inaccurate.

- Certain modifications were attempted on the OSA-R. An optical cell with smaller path length and new chemometric models were incorporated. The predictions from this modified OSA-R showed improvements, but V_{100} predictions were inaccurate.
- From the experiments performed, it was demonstrated that the finger print region of the IR spectrum is important in the accurate prediction of the desired properties. It was also determined that the original transmission based measurements could not be used.
- ATR IR spectra provide absorbances in a good working range throughout the "finger print" region, and are suitable for modeling purposes.
- The ATR IR technique is suitable for on-line applications; spectra obtained are reproducible and provide good model performance.
- Viscosity parameters namely, viscosity at 100 ^{0}F, 210 ^{0}F and viscosity Index have been successfully correlated to the ATR IR spectral data.
- Compositional characteristics obtained from ^{13}C NMR experiments also correlate well with the ATR IR spectra.
- For color, characterization using ATR IR spectra are not very feasible since aromatic and asphaltenes, which imparts color to the sample, have concentrations too low for IR measurement.

- UV/visible spectroscopy correlates to the color values for the samples provided with deviations averaging around 10%. The use of fresh sample set is expected to result in mark improvements in prediction of the color value.
- Alternative approaches to color measurement, such as tri-stimulus values of the sample from UV/visible spectroscopy may provide a better tool for on-line measurement.

Based on the experiments and results obtained in the experiments, it is very feasible to construct a prototype system for the rapid characterization of the heavy oil fractions in a petroleum refinery. The work presented here, demonstrates the successful modeling of the following physical and compositional properties of the heavy oil using ATR IR and UV/visible spectroscopy:

1. Viscosity parameters: Viscosity at 100 ^{0}F and 210 ^{0}F, Viscosity Index
2. Relative percentages of Paraffinic, Napthenic and Aromatics (PNA)
3. Color

Based on the results from this work, a prototype instrument can be built which integrates all the models derived in this work. A schematic of this prototype is illustrated in Figure.20. The prototype would feature both ATR IR and visible spectrometers. It would have a pump to facilitate the flow of the sample through these flow cells. The prototype would be designed initially for off-line measurements

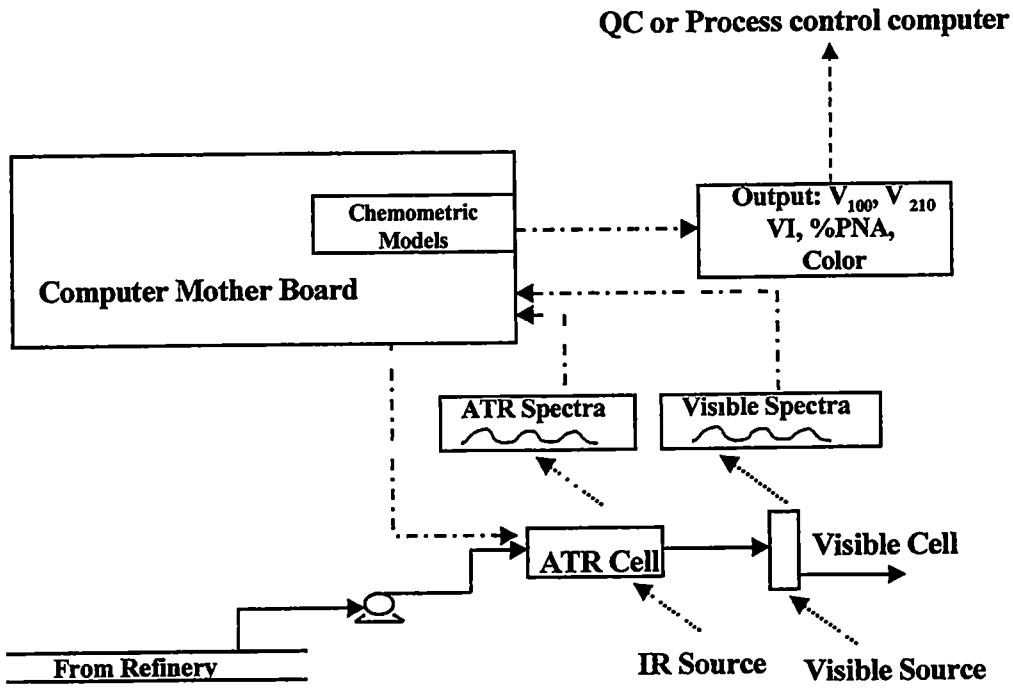


Figure 7.1 Schematic of the proposed prototype on-site analyzer.

but would have the potential to be adapted for on-line use. Collection of the spectral data is expected to take approximately 2 minutes. Once the spectral data are obtained, they would be processed by the chemometric models for the prediction of the physical and compositional characteristics of the sample. The whole process from the collection of the sample to the final predicted characteristics of the sample is estimated to take about 4 minutes.

References

References

1. Kinghorn, R. R. F. *An Introduction to the Physics and Chemistry of Petroleum.*, First ed.; John Wiley & Sons: 1983.

2. Speight James.G; Long, R. B.; Reynolds, J. G.; Khan, M. R.; Patmore, D. J.; Dolbear, G. E.; Mushrush, G. W. *Petroleum Chemistry and Refining*, First ed.; Taylor & Francis: 1998.

3. Gruse, W. A.; Stevens, D. R. *The Chemical Technology of Petroleum,* Second ed.; McGraw-Hill: 1942.

4. Gary, J. H.; Handwerk, G. E. *Petroleum Refining: Technology and Economics.*, First ed.; Marcel Dekker: 1984.

5. Allinson, J. P. *Criteria for Quality of Petroleum Products,* First ed.; John Wiley & Sons: 1973.

6. Fodor, G. E.; Kohl, K. B.; Mason, R. L. *Analysis of Gasoline by FTIR Spectroscopy.* Analytical Chemistry 68[1], 23-30. 1996.

7. Ramaswamy, Veda; Kothiyal, Vimal; Singh, Indra. D; Krishna, Rajamani. *Estimation of Total Aromatics in Kerosene Fractions by Infrared Spectroscopy -- II.* J.Chem.Tech.Biotechnol. 41, 255-259. 1988.

8. Kosal, Nejat; Bhairi, Abdullatif; Ali, Mohammed. Ashraf. *Determination of Hydrocarbon Types in Napthas, Gasolines and Kerosenes: A review and Comparative Study for Different Analytical Procedures.* Fuel 69[August], 1012-1019. 1990.

9. Caswell, K. Allen.; Glass, Thomas. E.; Swann. Madeline; Dorn, Harry. C. *Rapid prediction of various physical properties for middle distillate fuels*

utilizing directly coupled liquid chromatography/ super 1H nuclear magnetic resonance. Analytical Chemistry 61[3], 206-211. 1989.

10. Fodor, G. E.; Kohl, K. B. *Analysis of Middle Distillate Fuels by Midband Infrared Spectroscopy.* Energy & Fuels 7, 598-601. 1993.

11. Coates, J. P.; Setti, L. C. *Oils, Lubricants, and Petroleum Products: Characterization by Infrared Spectra*, First ed.; Marcel Dekker: 1985.

12. Wells, B. G. *Introduction to Molecular Theory and Experiments*, Academic Press.: 1970.

13. Skoog, D. A. *Principles of Instrumental Analysis.*, Third ed.; Saunders College Publishing: 1985.

14. Smith, A. L. *Applied Infrared Spectroscopy. Fundamentals, Techniques, and Analytical Problem Solving,* First ed.; John Wiley & Sons.: 1979.

15. Beebe, K. R.; Pell, R. J.; Seasholtz, M. B. *Chemometrics A Practical Guide,* First ed.; John Wiley & Sons: 1998.

16. Geladi, P.; Kowalski, B. R. *Analytica Acta* **1986,** *185.*

17. Martens, H.; Naes, T. *Multivariate Calibration,* Fisrt ed.; John Wiley & Sons: 1989.

18. Kvalheim, Olav. M.; Aksnes, Dagfinn. W.; Brekke, Trond, Eide, Magnus. O, Sletten, Einar. *Crude Oil Characterization and Correlation by Principal Component Analysis of ^{13}C Nuclear Magnetic Resonance Spectra.* Analytical Chemistry 57[14], 2858-2864. 1985.

19. Ali, Latif. H.; Al-Ghannam, Khalid. A.; Al-Rawi, Jasim. M. *Chemical Structure of Asphaltenes in Heavy Crude Oils Investigated by NMR.* Fuel 69[April], 519-521. 1990.

20. Wang; Zhendi; Fingas; Merv; Li, Ken. *Fractionation of Light Crude Oil and Identification and Quantitation of Aliphatic, Aromatic, and Biomarker Compounds by GC-FID and GC-MS, Part-I.* Journal of Chromotographic Science 32[September], 361-382. 1994.

21. Seifert, Wolfgang. K.; Teeter, Richard. M. *Identification of Polycyclic Napthenic, Mono-, and Diaromatic Crude Oil Carboxylic Acids.* Analytical Chemistry 42[2], 180-189. 1970.

22. Downare, Taggart. D.; Mullins, Oliver. C. *Visible and Near-Infrared Fluoroscence of Crude Oils.* Applied Spectroscopy 49[6], 754-764. 1995.

23. Claudy; Pierre; Letoffe; Jean-Marie; Chague; Benoit; Orrit, Jean. *Crude Oil and their Distillates: Characterization by Differential Scanning Calorimetry.* Fuel 67[January], 58-61. 1988.

24. Felix, G.; Thoumazeau, E.; Colin, J. M. J.Liq.Chromotography 10[10], 2115-2132. 1987.

25. Orbey, H.; Sandler, S. I. Can.J.Chem.Eng. 71[3], 565-573. 1993.

26. Maidoyne, A.; Puttagunta, V. R,; Singh, B. Chem.Eng.Commun. 122, 195-199. 1993.

27. Yokayama, S.; Uchino, H.; Tanabe, K.; Satou, M.; Sanada, Y. Fuel 66[10], 1330-1335. 1987.

28. Pruski, M,; Gerstein, B. C.; Michel, D. *NMR of Petroleum Cokes II: Studies by High Resolution Solid State NMR of ^{1}H and ^{13}C* Carbon 32[1], 41-49. 1994.

29. McAskill, Noel. A. *Near-Infrared Photoacoustic Spectroscopy of Coals and Shales.* Applied Spectroscopy 41[2], 313-317. 19987.

30. Bartlett, C. J. S. *The Relationship Between Aromatic Content and Specification Parameters in Diesel Fuels.* Petroleum Review [February], 84-85. 1990.

31. American Society for Testing and Materials. *ASTM test method designation D1319-93.* Annual Book of ASTM Standards, Philadelphia:1995.

32. Chung, W. M.; Wang, Q.; Sezerman, U.; Clarke, R. H. *Analysis of Aviation Turbine Fuel Composition by Laser Raman Spectroscopy.* Applied Spectroscopy 45[9], 1527-1532. 1991.

33. Seasholtz, M. B.; Archibald, D. D.; Lorber, A.; Kowalski, B. R. *Quantative Analysis of Liquid Fuel Mixtures with the Use of Fourier Transform Near IR Raman Spectroscopy.* Applied Spectroscopy 43[6], 1067-1072. 1989.

34. Williams, Kenneth. P. J.; Aries, Rupert. E.; Cutler, David. J.; Lidiard, David. P. *Determination of Gas Oil Cetane Number and Cetane Index Using Near-Infrared Fourier Transform Raman Spectroscopy.* Analytical Chemistry 62[23], 2553-2556. 1990.

35. Cooper, John. B.; Wise, Kent. L.; Groves, James.; Welch, William. T. *Determination of Octane Numbers and Reid Vapor Pressure of Commercial Petroleum Fuels Using FT-Raman Spectroscopy and Partial Least-Squares Regression Analysis.* Analytical Chemistry 67[22], 4096-4100. 1995.

36. Cooper, J. B.; Flecher, P. E.; Vess, T. M.; Welch, W. T. Applied Spectroscopy 49, 586-592. 1995.

37. Sri'ca, Vlasta.; Mühl, Jasenka.; Jednacak, Mir.; and Duric, Anka. *Determination of Hydrocarbon Type Distribution of Coking Gasolines by NMR Spectrometry.* Fuel 72[6], 775-778. 1991.

38. Singh, Himmat.; and Srivastava, S. P. *Average Molecular Structures of Lubricating Oil Base Stocks in Relation to their Degree and Type of Refining.* Petroleum Review [June], 41-45. 1987.

39. Brant, W. C.; Kiviat, F. E. *Proceedings of the 31st annual ISA analysis instumentation symposium presented at DIGITECH '85, Northeastern Conference and exhibit on industrial instrumentation control,* May 14-16, 1985, Boston, 1985 85; ISA; 35-41.

40. Wiseman, Murray.; Ah-Sue, Alan. *Monitoring Oil Degradation Using FTIR Analysis.* Lubrication Engineering 48[3], 236-241. 1992.

41. Stuart, A. D.; Trotman, S. M.; Doolan, K. J.; Fredericks, P. M. *Spectroscopic Measurement of Used Lubricating Oil Quality* Applied Spectroscopy 43[1], 55-60. 1989.

42. Kushnarev, D. F.; Afonina, T. V.; Demidenko, K. A.; Bezhanidze, A. M.; Dolbanova, T. A.; Kalabin, G. A. *Investigation of Base Oils by NMR Spectroscopy* Chemistry and Technology of Fuels and Oils 25[1-2], 48-52. 1989.

43. Paschke, A.; Herbel, W.; Steinhart, H.; Franke, S.; Franke, W. J.High Resolut Chromatogr. 15[12], 827-833. 1992.

44. Navarro Frometa, A. E. Analyst 119[5], 987-989. 1994.

45. Singh, I. D.; Aloopwan, M. K. S.; Chaudhary, G. S.; Singh, H. Fuel 71[11], 1335-1337. 1992.

46. Yen, Teh Fu.; Wu, Wen Hui.; Chilingar, George. V. *A Study of the Structure of Petroleum Asphaltenes and Related Substances by Infrared Spectroscopy* Energy Sources 7[3], 203-235. 1984.

49. Khorasheh, Farhad.; Gray, Murray. R.; Lana, Ivo. G. Dalla. *Structural Analysis of Alberta Heavy Gas Oils.* Fuel 66[April], 505-511. 1987.

48. Kotlyar, Luba. S.; Ripmeester, John. A.; Sparks, Bryan. D.; Montgomery, Douglas. S. *Characterization of Oil Sand Solids Closely Associated with Athabasca Bitumen* Fuel 67[June], 808-814. 1988.

49. Misbah-ul-Hasan; Siddiqui-M-Nahid; Arab-M. *Separation and Characterization of Asphaltenes from Saudi Arabian Crudes* Fuel 67[August], 1131-1134. 1988.

50. Giavarini-Carlo; Vecchi-Carmen. *Characterization of visbreaker bitumens by NMR spectroscopy.* Fuel 66[June], 868-869. 1998.

51. Kaihara, Mikio.; Mametsuka, Hiroaki.; Gunji, Naoki.; Gohshi, Yohichi. *Novel Characterization Techniques for Pitches and Coal Slurries using Fourier Transform Infrared Spectrometry.* Fuel 70[August], 931-933. 1991.

52. Ram, Shankar.; Saraswat, Devesh. K.; Narayan, Kumar. A. *Spectroscopic Studies of Athabasca Oil Sands.* Fuel 69[April], 512-515. 1990.

53. Moschopedis, S. E; Speight, J. G. Fuel 55, 187. 1976.

54. Philip, C. V.; Bullin, J. A.; Glover, C. J.; Davison, R. R. *Preprints,* 1989 4-9-1989; ACS, Division of Petroleum Chemistry; 311-15.

55. Shoolery, J. N.; Budde, W. L. Analytical Chemistry 48[11], 1458. 1976.

56. Gillet, S.; Delpuech, J. J.; Valentin, P.; Escalier, J. C. Analytical Chemistry 52[6], 813. 1980.

57. Holak, T. A.; Ajsbesm, D. W.; Stocker, M. Analytical Chemistry 56[4], 725. 1984.

58. Ali, M. F.; Bukhari, A. *Preprints* , 1989 4-9-1989; ACS, Division of Petroleum Chemistry; 306-09.

59. Yokoyama, Susumu.; Bodily, David. M.; Wiser, Wendell. H. *Structural Characterization of Coal-Hydrogenation Products by Proton and C-13 NMR.* Fuel 58[March], 162-170. 1979.

60. Haley, Graeme. A. *Molecular and Unit Sheet Weights of Asphalt Fractions Separated by Gel Permeation Chromotography* Analytical Chemistry 43[3], 371-375. 1971.

61. Hayes, Paul. C.; Anderson, Steven. D. *Hydrocarbon Group Type Analyzer System for the Rapid Determination of Saturates, Olefins, and Aromatics in Hydrocarbon Distillate Products.* Analytical Chemistry 58[12], 2384-2388. 1986.

62. Ramaswamy, Veda.; Singh, Indra. D.; Krishna, Rajamani. *Characterization of Vacuum Gas Oils from North Gujarat Crude Mix* Indian Journal of Technology 27[February], 85-88. 1989.

63. Shui, Hengfu.; Shen, Benxian.; Gao, Jinsheng. *Study of the Structure of Heavy Oils.* Petroleum Science and Technology 15[7&8], 595-610. 1997.

64. Ali, M. Farhat.; Bukhari, Ahmed.; Hasan, Misbah-ul. *Structural Characterization of Arabian heavy Crude Oil Residue.* Fuel Science and Technology Int'L 7[8], 1179-1208. 1989.

65. Netzel, Daniel. A.; Turner, Thomas. F. *A Correlation of United States Tar Sand Bitumen Viscosities with NMR Spectroscopic Parameters* Fuel Science and Technology Int'L 8[4], 379-403. 1990.

66. Bukka, K.; Miller, J. D.; Hanson, F. V.; Misar, M.; Oblad, A. G. Fuel 73[2], 257-268. 1998.

67. Zerila, Tiziana; Pinelli, Giacomo. *A New Approach to the Determination of Saturates in Heavy Petroleum Products.* Fuel 72[4], 505-509. 1993.

68. Speight James.G. *Application of Spectroscopic Techniques to the Structural Analysis of Petroleum.* Applied Spectroscopy Reviews 29[3&4], 269-307. 1994.

69. Yamashita, G. T.; Saetre, R.; Somogyvari, A. *Preprints*, 1989 4-9-1989; ACS, Division of Petroleum Chemistry; 301-09.

70. Michel, D.; Pruski, M.; Gerstein, B. C. *NMR of Petroleum Cokes I· Relaxation Studies and Quantitave Analysis of Hydrogen by Magnetic Resonance.* Carbon 32[1], 31-40. 1994.

71. Dosseh, Gilberte.; Rousseau, Bernard.; Fuchs, Alan. H. *Identification of Aromatic Molecules in Intermediate Range Boiling Crude Fractions by 2D NMR Spectroscopy.* Fuel 70[May], 641-646. 1991.

72. Speight James.G. *The Application of Spectroscopic Techniques to the Structural Analysis of Coal and Petroleum.* Applied Spectroscopy Reviews 5[2], 211-264. 1971.

73. Haaland, David. M.; Thomas, Edward. V. *Partial Least-Squares Methods for Spectral Analyses. 2. Application to Simulated and Glass Spectral Data.* Analytical Chemistry 60[11], 1202-1208. 1988.

Vita

Kislaya Gautam was born in Patna, India on July 2, 1973. He attended high school at St. Michael's High School, Patna, India. He joined Indian Institute of Technology, Kanpur, India in August 1993, where he received the Bachelor of Technology degree in Chemical Engineering in May 1997. In August 1997, he joined The University of Tennessee, Knoxville for the Master of Science program in Chemical Engineering.